

UNCLASSIFIED



Australian Government
Department of Defence
Defence Science and
Technology Organisation

An Investigation into the Effects of Roll Gyradius on Experimental Testing and Numerical Simulation: Troubleshooting Emergent Issues

Edward Dawson

Maritime Division
Defence Science and Technology Organisation

DSTO-TN-1402

ABSTRACT

This report presents the analyses, results and recommendations of an investigation into the specification and determination of a platform's roll radius of gyration and its influence on the measured or predicted roll response of a maritime platform. The investigation and report seek to resolve known deficiencies in the specification and determination of roll radius of gyration and provide direct guidance and supporting information to the experimenter and analyst to support ship motion analysis. Three solution sets were developed based on the results of the investigation. The solutions include: the establishment of a method of specifying roll radius of gyration requirements; the development of a decision tree tool to guide the analyst to the appropriate method of determining the roll radius of gyration; and a set of system level technology solutions that enable the roll radius of gyration to be determined for model scale, full scale and virtual maritime platforms.

RELEASE LIMITATION

Approved for public release

UNCLASSIFIED

UNCLASSIFIED

Published by

*Maritime Division
DSTO Defence Science and Technology Organisation
506 Lorimer St
Fishermans Bend, Victoria 3207 Australia*

*Telephone: 1300 333 362
Fax: (03) 9626 7999*

*© Commonwealth of Australia 2015
AR-016-225
January 2015*

APPROVED FOR PUBLIC RELEASE

UNCLASSIFIED

An Investigation into the Effects of Roll Gyradius on Experimental Testing and Numerical Simulation: Troubleshooting Emergent Issues

Executive Summary

The numerical ship motion simulation and analysis tools used by the Defence Science and Technology Organisation (DSTO) are an efficient and effective means to determine and evaluate the motion performance of a platform operating in a seaway. However, their accuracy and applicability are strongly influenced by the initialisation data input by the user. The use of incorrect data or data used incorrectly in the initialisation phase can result in misleading simulation outputs. A comparison between the experimental and numerical simulation results conducted by Hill et al. [1] in their investigation into the motion response of naval landing craft showed a significant difference in the roll motion frequency. Hill et al. [1] attributed this discrepancy to the numerical simulation software used and possible limitations in the calculation of added mass. Further investigations into the issues observed by Hill et al. [1] were conducted by DSTO and the outcomes are presented in this report.

On investigation it was determined that the fundamental cause of the discrepancy observed by Hill et al. [1] was that they used a roll radius of gyration (roll gyradius) input in the software simulation that had been determined experimentally and did not include the effects of hydrodynamic added mass. The software used by Hill et al. [1] requires the roll gyradius to include the effects of added mass. So although the roll gyradius measured by Hill et al. [1] was accurate, it was not appropriate for use as an input to their simulation, at least not without a modification to include the effects of added mass. A review of the theoretical formulations of roll motion has confirmed that the discrepancy is due to the omission of added mass effects in the simulation input data. Identifying the direct cause of the discrepancy prompted a more considered assessment of the issues experienced by Hill et al. [1]. It was concluded that the causal factors that led to the incorrect data being used in the simulation were:

1. The specification of the roll gyradius data requirement was ambiguous.
2. No formalised or traceable guidance was available to the experimenter or analyst regarding the specification of the required roll gyradius data and which method to use to determine the appropriate roll gyradius.
3. There was limited or no information that described the quality of the methods available to determine the roll gyradius.

UNCLASSIFIED

A qualitative and quantitative review of the available methods of determining the roll gyradius of a platform model, whether physical or virtual, has been conducted to address these issues and support the development of a set of solutions. The results of the review indicate that the most appropriate method for determining the roll gyradius of a physical model is to conduct an in-water roll decay test using a non-contact motion sensing system. This method produces a result that includes the effects of added mass. Where a roll decay test cannot be conducted, the roll frame method is an effective alternative and has been shown to provide accurate data. However, additional effort is required to determine the added mass component using strip theory based analysis software. In cases where only a virtual model of the platform exists, a coupled computational method using computer aided design solid modelling and strip theory based analysis software can be used to determine the roll gyradius.

A function and performance evaluation of the existing large and small roll frame devices operated by the Australian Maritime College and used by DSTO has indicated that under appropriate loading conditions the small roll frame will produce an accurate measurement of a model's roll gyradius. However, structural limitations inherent in the roll frame design have been shown to result in frame deformation when under heavy model loads. The deformation will cause misalignment and probably lead to an adverse level of error in the measurement result. These issues can be resolved through further analysis and design modification.

The results of the investigations presented in this report have been used to develop a solution to address the issues encountered by Hill et al. [1] and provide guidance for future experimental and numerical investigations. The solution comprises:

1. A textual template for preparing a requirements statement to define the roll gyradius of a platform and load condition.
2. A Decision Tree to inform and guide the experimenter and analyst as to the most appropriate method of determining the roll gyradius of a platform model, whether physical or virtual.
3. Three technology and process oriented system level solutions to determine the roll gyradius of a platform.

By implementing the research outcomes and solutions detailed in this report DSTO and the Australian Maritime College will be able to provide additional assurance of the quality of the research conducted to evaluate maritime platform ship motions in support of the Royal Australian Navy and broader Australian Defence Organisation.

UNCLASSIFIED

UNCLASSIFIED

Author

Edward Dawson Maritime Division

Edward Dawson is a Research Scientist with the Australian Defence Science and Technology Organisation. He holds a Bachelor of Engineering (Naval Architecture) and a Master of Philosophy (Hydrodynamics) from the University of Tasmania. Prior to joining DSTO Edward worked in the Australian commercial and Defence maritime industry as a consulting engineer. In his current role, Edward is principally involved in the weapons and combat systems effectiveness and analysis technology domain.

UNCLASSIFIED

UNCLASSIFIED

This page is intentionally blank

UNCLASSIFIED

Contents

ACRONYMS AND ABBREVIATIONS

NOMENCLATURE

AXIS CONVENTION

1. INTRODUCTION.....	1
1.1 Study Objectives and Outcomes.....	2
2. THEORETICAL BACKGROUND.....	4
2.1 Roll Period, Roll Gyradius and Added Mass	4
3. METHODS TO DETERMINE ADDED MASS AND ROLL GYRADIUS.....	7
3.1 Determining Added Mass in Roll	7
3.2 Roll Gyradius: Discrete Element Method	7
3.3 Roll Gyradius: Computer Aided Design (CAD) Method.....	8
3.4 Roll Gyradius: Physical Measurement Methods	8
3.4.1 Compound Pendulum.....	9
3.4.2 Roll Frame.....	10
3.4.3 Roll Decay Test	11
3.5 Summary.....	13
4. SENSITIVITY STUDIES AND UNCERTAINTY ANALYSES	14
4.1 Sensitivity Study.....	14
4.1.1 Roll Frame: Roll Gyradius.....	15
4.1.2 Inclining Test: Metacentric Height.....	16
4.1.3 Roll Decay Test: Roll Gyradius.....	17
4.2 General Uncertainty Analyses.....	18
4.2.1 Roll Frame Test: Roll Gyradius (in air).....	18
4.2.2 Inclining Test: Metacentric Height.....	19
4.2.3 Roll Decay Test: Roll Gyradius (in water).....	20
4.3 Discrete Element Method: Discretization Sensitivity Analysis.....	21
4.4 Summary.....	22
5. SOLUTIONS	24
5.1 Procedural Guidance	24
5.2 System Level Solutions.....	25
6. CONCLUDING REMARKS	28
7. ACKNOWLEDGEMENTS	29

8. REFERENCES	30
APPENDIX A: DECISION TREE: METHOD TO DETERMINE A PLATFORM'S ROLL GYRADIUS.....	31
APPENDIX B: ROLL FRAME FUNCTION AND PERFORMANCE EVALUATION	34
B.1. Test Setup, Procedure and Results.....	35
B.2. Comparison with CAD Method	41
B.3. Design Issues	41
B.4. Summary	49
APPENDIX C: GENERAL UNCERTAINTY ANALYSES: DERIVATION OF ERROR PROPAGATION EQUATIONS.....	50
C.1. Roll Frame Test: Roll Gyradius (in air).....	50
C.2. Inclining Test: Metacentric Height	50
C.3. Roll Decay Test: Roll Gyradius (in water).....	51

Acronyms and Abbreviations

AMC	Australian Maritime College
BNC	Bayonet Neill-Concelman
CAD	Computer Aided Design
DAQ	Data acquisition
DC	Direct current
DSTO	Defence Science and Technology Organisation
HP	Hewlett Packard
NCMEH	National Centre for Maritime Engineering and Hydrodynamics
OFAT	One factor at a time
PC	Personal computer
SHS	Square hollow section
XCG	Location of the centre of volume or mass in the longitudinal axis
YCG	Location of the centre of volume or mass in the transverse axis
ZCG	Location of the centre of volume or mass in the vertical axis

Nomenclature

A_{xx}	Added mass in roll (kg-m ²)
b	Damping (kg-m)
c	Stiffness (N-m/rad)
g	Acceleration due to gravity [9.81] (m/s ²)
GM_T	Transverse metacentric height [$GM_T = KM_T - KG$] (m)
h	Distance from compound pendulum pivot point and model centre of gravity (m)
h_F	Distance from compound pendulum pivot point and compound pendulum frame centre of gravity (m)
h_P	Distance from roll frame pendulum pivot point and roll frame centre of gravity (m)
i	Element number (i th element)
I'_{xx}	Virtual roll moment of inertia (kg-m ²)
I_F	Moment of inertia of compound pendulum [frame only] (kg-m ²)
I_{System}	Moment of inertia of compound pendulum system [frame and model] (kg-m ²)
I_{xx}	Roll mass moment of inertia (kg-m ²)
k'_{xx}	Added mass roll radius of gyration (m)

k''_{xx}	Virtual roll radius of gyration (m)
KG	Vertical location of the centre of gravity [above the keel] (m)
KM_T	Transverse metacentre (m)
k_{xx}	Roll radius of gyration (m)
M	Combined mass of the platform and inclining weight (kg)
m	Mass of model (kg)
m_F	Mass of compound pendulum frame (kg)
m_m	Mass of model (kg)
m_P	Roll frame pendulum mass (kg)
T_n	Natural period (sec)
T_ϕ	Natural roll period (sec)
T_d	Damped roll period (sec)
V	Volume (m ³)
w	Weight of element (kg)
x	Principal axis in longitudinal direction (positive forward)
y	Principal axis in transverse direction (positive to port)
z	Principal axis in vertical direction (positive down)
Δ	Displacement (or mass) of platform (kg)
Δ'	Virtual displacement (or mass) of ship [$\Delta' = \Delta + \delta\Delta$] (kg)
δI_{xx}	Added mass component of roll mass moment of inertia (kg-m ²)
$\delta\Delta$	Added mass component of displacement (or mass) of ship (kg)
θ	Angle of incline (deg)
ν	Decay constant
π	Pi [3.1416] (constant)
ω_n	Natural frequency (rad/sec)

Axis Convention

x	Longitudinal direction, stern to bow, positive forward
y	Transverse direction, port to starboard, positive to starboard
z	Vertical direction, baseline to deck, positive upwards
ϕ	Rotation about x axis, positive roll to port

1. Introduction

Recent research into the deep water roll behaviour of landing craft hull forms using numerical and experimental methods, conducted by Hill et al. [1], has highlighted issues with the application of existing experimental procedures and equipment to determine the roll gyradius of a physical ship model. When completing a comparison between the experimentally measured and numerically predicted roll decay motion Hill et al. [1] observed a significant phase difference in the roll motion frequency. An example of the observed phase difference is shown in Figure 1. To enable the validation of numerical ship motion prediction tools and conduct analyses of platform motion behaviour, it is imperative that the user input platform geometry and mass properties are correct. Inaccurate input data can result in inaccurate and misleading ship motion simulation results.

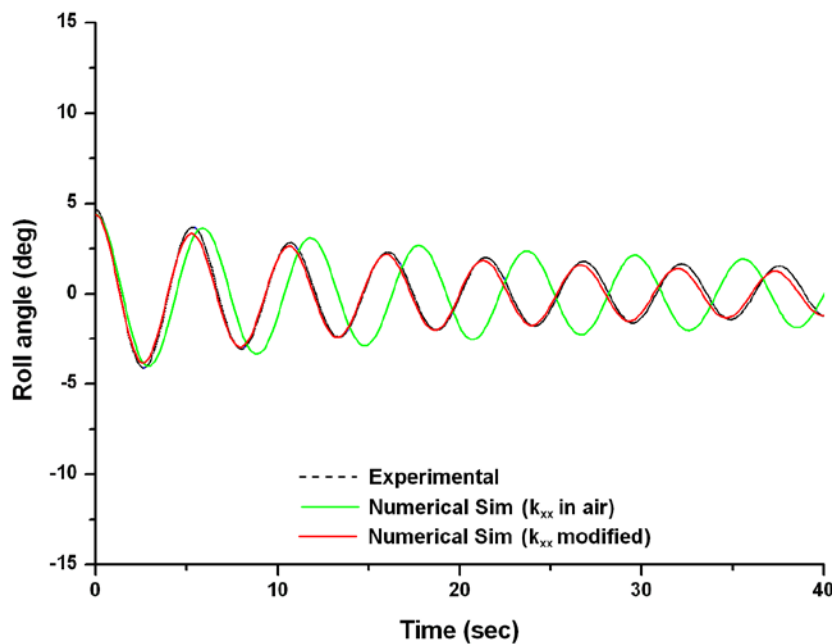


Figure 1 Comparison of experimental and numerical roll decay data for a generic landing craft hull form (Adapted from Hill et al. [1]).

Investigations by the author have indicated that the discrepancy observed by Hill et al. [1] is likely to be attributed to the values of the metacentric height (GM_T) or the roll gyradius (k_{xx}) or both that were input as initial conditions in Hill et al.'s [1] numerical simulation. Furthermore, the cause of the difference in the roll gyradius is likely to be due to the absence of added mass in the measurement of the roll gyradius of the experimental model.

Hill et al.'s [1] experiments were conducted at the Australian Maritime College (AMC) in Launceston, Tasmania. The current methods employed by the AMC to determine the metacentric height and the roll gyradius of a physical model are to conduct an in-water inclining test and a free decay oscillation test using a roll frame, respectively. In both

instances these methods are appropriate for determining the physical characteristics of the model; however, by virtue of the roll frame measurement procedure and set-up, the measured roll gyradius does not account for the added mass component of the model when oscillating in a viscous liquid. Consequently, the roll frame roll gyradius cannot be used as an initial condition in numerical simulations where the modelled platform is floating in a liquid; at least not without due consideration of the platform's added mass. The effect of the added mass on the roll moment of inertia and consequently roll period is shown in Figure 1 where the 'in air' roll gyradius produces a response with a longer period of oscillation than that measured for the model oscillating in fresh water. As discussed by Hill et al. [1], the experimental method adopted in their investigation involved using the roll frame to determine the roll gyradius of the physical models. Nonetheless, the simulation software used by Hill et al. [1] requires an 'in-water' roll gyradius as an initial input.

On further investigation it was concluded that the fundamental issues encountered by Hill et al. [1] were:

1. The specification of the required model roll gyradius was ambiguous. This is likely to be attributed to the lack of information supporting the principal requirement and the intended application of the test results. The specification of the platform roll gyradius did not contain specific information to qualify the conditions under which the roll gyradius value pertained.
2. An explicit statement of guidance did not exist to direct the experimenter/analyst to the appropriate method for determining the roll gyradius of their platform with respect to their intended analyses.
3. There was limited information describing the quality of the methods available to determine the roll gyradius of the platform. Due to this lack of information the experimenter/analyst was not able to make an informed decision as to which test method to use.

In response to the issues raised in this investigation, a method of accurately determining the mass properties of physical models and full scale platforms oscillating in a liquid is required to enable the measurement or prediction of platform roll response using experimental methods or numerical simulation tools, respectively.

1.1 Study Objectives and Outcomes

The principal objectives of this study are to:

1. Qualify the assertion that the discrepancy observed by Hill et al. [1] is due to the use of a roll gyradius that does not include the effects of hydrodynamic added mass.
2. Investigate the effectiveness and accuracy of the existing methods to measure or predict the roll gyradius of a physical or virtual model.
3. Establish an experimental approach to measure the roll gyradius of a physical model in calm water.

4. Establish a method for predicting the roll gyradius, and hence roll period, for a physical model (and full scale ship) without need for experiment.
5. Quantitatively and qualitatively evaluate the performance of the existing roll frame device and test method used to determine the roll gyradius of a physical model.

The results of the roll frame function and performance evaluation are presented in Appendix B.

The outcomes of this research will include, but not be limited to:

1. A quantitative evaluation of the prominent and applicable methods of determining the roll gyradius of a physical or virtual model.
2. The proposal of a method for determining the roll gyradius of a platform without need for experiment.
3. A solution set to overcome the issues experienced by Hill et al. [1] and support the future needs of experimenters and analysts involved in the analysis of maritime platform motion response.

2. Theoretical Background

This section presents the theoretical formulation of the roll gyradius of a floating body and the inter-relationship between roll gyradius, added mass and roll period.

2.1 Roll Period, Roll Gyradius and Added Mass

It is widely reported that the natural roll period (T_ϕ) of a ship or floating platform is a function of its roll gyradius (k_{xx}) and transverse metacentric height (GM_T), see for example [2-5]. The theoretical relationship between the un-damped roll period, roll gyradius and metacentric height is presented in Equation 1.

$$T_\phi = \frac{2\pi \cdot k_{xx}}{\sqrt{g \cdot GM_T}} \quad \text{Equation 1}$$

This relationship is considered to exist where the roll motion is isochronous (of equal interval) and the angle of roll (ϕ) is no greater than ± 10 degrees [5]. It is noted that this formulation does not explicitly account for the effects of added mass (the virtual mass of the floating body). Due to the effects of added mass the roll gyradius of a floating platform will be greater than the roll gyradius predicted or measured in air or independent of fluid interaction. Considering the effects of added mass, the relationship between the platform's roll gyradius and mass can be derived and is presented in Equation 2.

$$k_{xx} = \sqrt{\frac{I_{xx} + A_{xx}}{\Delta}} \quad \text{Equation 2}$$

It is the roll added mass (A_{xx}) component that causes the platform's roll gyradius measured in air to be different to the roll gyradius of the platform when oscillating in water. The difference between the 'in air' and 'in water' roll gyradius results in a proportional difference in the roll period. Rawson and Tupper [5] report that the effect of added mass can lead to an increase in roll gyradius of approximately 10 to 30 percent; however, this varies significantly with hull form geometry and platform type.

Bhattacharyya [2] provides a more detailed derivation and explanation of the effect of added mass. In this instance, the virtual mass moment of inertia of the ship is represented by I'_{xx} as is shown in Equation 3. Here the added mass component is represented by $\delta\Delta$.

$$I'_{xx} = \frac{\Delta}{g} k_{xx}^2 + \frac{\delta\Delta}{g} k_{xx}^2 = \frac{\Delta'}{g} k_{xx}^2 \quad \text{Equation 3}$$

Bhattacharyya [2] also reports that the added mass moment of inertia in roll for a platform is approximately 20 percent of the displacement. Alternatively, the virtual mass moment of inertia relationship can be represented in terms of a virtual roll gyradius as shown in Equation 4.

$$I'_{xx} = \frac{\Delta}{g} (k_{xx}^2 + k_{xx}'^2) = \frac{\Delta}{g} k_{xx}''^2 \quad \text{Equation 4}$$

The virtual roll gyradius (k_{xx}'') is typically presented as a percentage of the platform's maximum waterline beam (B) and is frequently reported as being in the region of $0.30B \leq k_{xx}'' \leq 0.45B$ depending on the platform type [2]. Since the virtual roll gyradius is directly related to the added mass of the body, Equation 2 can be represented as Equation 5.

$$k_{xx}'' = \sqrt{\frac{I_{xx} + A_{xx}}{\Delta}} \quad \text{Equation 5}$$

It is the virtual roll gyradius that will provide the correct roll period when comparing the calculated value (Equation 1) with a physical measurement conducted in water.

The theoretical representations presented so far do not explicitly account for the effects of damping on the roll response of the platform. For completeness, the relationship between the un-damped and damped roll period and gyradius is presented here.

As part of the solution to the equation of motion of floating body rolling in calm water, the roll velocity dependent damping term (b) is represented by Equation 6.

$$2\nu = \frac{b}{I'_{xx}} \quad \text{Equation 6}$$

Here b is the roll velocity related damping term in the equation of motion (Equation 7).

$$I'_{xx} \frac{d^2\phi}{dt^2} + b \frac{d\phi}{dt} + \Delta \cdot GM_T \phi = 0 \quad \text{Equation 7}$$

The damped frequency of oscillation in roll is related to the un-damped frequency of oscillation as shown in Equation 8.

$$\omega_d = \sqrt{\omega_\phi^2 - \nu^2} \quad \text{Equation 8}$$

Consequently, the damped roll period becomes:

$$T_d = \frac{2\pi}{\sqrt{\omega_\phi^2 - \nu^2}} \quad \text{Equation 9}$$

Bhattacharya [2] reports that the effect of damping is to increase the roll period, but also that this effect is typically negligible due to the relative magnitude of the incident roll damping experienced by typical ship shaped platforms. It is therefore acceptable to consider the damped and un-damped roll periods to be approximately equal.

Based on the theoretical formulations presented here and the influence of added mass on roll period discussed by Rawson and Tupper [5] and Bhattacharyya [2] it is evident that the discrepancy observed by Hill et al. [1] is most likely to be attributed to the use of an 'in air' roll gyradius as an input into an 'in water' numerical simulation. The alternative source of discrepancy is the experimental error in the measurements of the roll gyradius and metacentric height. While these sources of error are not considered to be significant enough to cause the discrepancy observed by Hill et al. [1], an evaluation of the magnitude of the experimental error was completed and is presented in § 4.

3. Methods to Determine Added Mass and Roll Gyradius

Several methods exist to determine the principal gyradii of a body and the added mass that is induced by its oscillatory motion in a fluid. The following sections provide an overview of the methods that are currently used by experimentalists and analysts.

3.1 Determining Added Mass in Roll

Two common methods for determining the added mass of a body oscillating in a liquid are to make direct measurements (experimentally) or by a numerical method known as strip theory. Strip theory methods use either the Frank Close Fit or Lewis Form formulations to compute the added mass of a specific hull geometry. Modern numerical methods and computer systems have allowed the strip theory approach to be applied to most hull types and geometries to calculate the added mass components quickly and effectively. For a detailed description of the application of strip theory see, for example, [2, 3, 6]. The relative low cost and timeliness of the strip theory method makes it the preferred choice in comparison to conducting an experiment, at least for the majority of applications.

Typically, all frequency domain seakeeping software codes will calculate the added mass of the hull geometry for a range of encounter frequencies. Therefore, it is a relatively straight forward process to determine the roll added mass (A_{xx}) of a platform with a known hull geometry. More advanced programs such as the SHIPMO2000 component of the FREDYN [7] time-domain ship motion analysis program can compute the added mass of a platform in deep and shallow water conditions. Research conducted by Inglis and Price [8] has shown that the added mass of a platform will differ between deep and shallow water conditions with the general behaviour indicating an increase in added mass with a reduction in water depth.

3.2 Roll Gyradius: Discrete Element Method

The discrete element method used to calculate a platform's roll gyradius involves taking the first mass moment of each mass element on-board the platform about the global centre of gravity. That is, the platform is discretized into elements of mass and the moment of these elements are taken about the platform's centre of gravity in terms of the relative lateral and vertical distance to the elements' individual centre of gravity [2]. This procedure is best represented by Equation 10 where w_i is the mass of an individual element and y_i and z_i are the lateral and vertical distances between the element's centre of mass and the platform's global centre of gravity, respectively.

$$k_{xx} = \sqrt{\frac{\sum w_i (y_i^2 + z_i^2)}{\Delta}} \quad \text{Equation 10}$$

It should be noted that this method will provide the roll radius of gyration independent of the environment in which it is operating and therefore does not account for added mass. This method can be used for any size platform from model to full scale. However, its accuracy is constrained by the level of discretization and the measurement uncertainty of the weight and distance of each of the elements.

3.3 Roll Gyradius: Computer Aided Design (CAD) Method

There are currently many computer aided design (CAD) software programs that include routines (commands) for calculating the area, volume and mass properties of surface and solid model objects. The Rhinoceros 3D [9] CAD software program is used in this study to investigate its application and ability to calculate the gyradii of solid object CAD models representing physical models. The method to determine the mass properties of a solid object programmed within the Rhinoceros 3D CAD software involves the use of surface integrals and numerical integration techniques. In this instance, the Romberg integration method is used as it also provides an estimate of the integration error. The volume of each object is calculated using Stokes' theorem to represent the volume as the surface integral of the object's boundary [10].

The volume moment of inertia of a body about its own axis, relative to a global axis, is defined by Equation 11. In this instance it is assumed that the body is aligned such that its roll rotational motion is about the x axis. In Equation 11 the first two integrals represent the second moment of inertia, the second two integrals represent the first moment of inertia and the final term represents the parallel axis transformation. The volume moment of inertia has the units of m^5 .

$$I_x = \int_V y^2 dV + \int_V z^2 dV - 2y_0 \int_V y \cdot dV - 2z_0 \int_V z \cdot dV + V(y_0^2 + z_0^2) \quad \text{Equation 11}$$

The roll gyradius of the body is simply calculated using the volume moment of inertia about the x axis and the total volume of the body (Equation 12). In this instance, the calculation is independent of density. If multiple components of varying density are modelled, then either separate calculations would be required for each set of objects with a common density or a mass specific routine should be used.

$$k_{xx} = \sqrt{\frac{I_x}{V}} \quad \text{Equation 12}$$

3.4 Roll Gyradius: Physical Measurement Methods

Common methods to physically measure roll gyradius are to use either a compound pendulum or a roll frame. These devices are very practical for determining the roll moment of inertia of scale models. An alternate method is to conduct an unconstrained roll decay test with the model floating in water. The difference between the

pendulum/frame and roll decay test is that the later method accounts for the effects of hydrodynamic added mass.

3.4.1 Compound Pendulum

In the case of the compound pendulum the ship model is held in a stiff but light frame which is suspended centrally below a pivot point as shown in Figure 2. The distance from the model's vertical centre of gravity and the pivot point is denoted by h . The mass, centre of gravity and moment of inertia of the frame must also be determined. The frame's moment of inertia is determined by conducting the free oscillating test with the frame only.

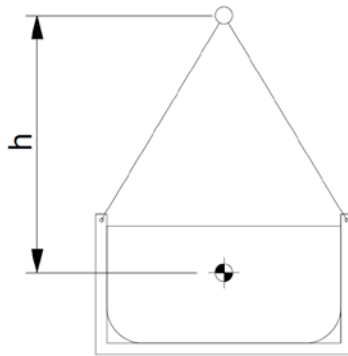


Figure 2 Compound Pendulum with ship model (End View) [4].

Then the frame and the model are displaced by a small angle about the pivot point and released. As the frame and frame with model configurations oscillate freely from side to side the natural period of oscillation is measured by recording the time for the frame to complete a set number of oscillations [4]. Lloyd [4] suggests ten oscillations; however, if a precise and accurate time measurement system is used the number of oscillations may be reduced. The initial angle to which the frame is rotated may have an effect on the accuracy of the measurement. As with many measurements it would be prudent to repeat the process several times. The roll radius of gyration is determined by the following relationship as presented by Lloyd [4].

Using the parallel axis theorem, the combined moment of inertia of the frame and model system is:

$$I_{System} = mk_{xx}^2 + mh^2 + I_F \quad \text{Equation 13}$$

The stiffness of the compound pendulum is:

$$c = g(mh + m_F h_F) \quad \text{Equation 14}$$

The natural frequency of oscillation of the system is:

$$\omega_n = \frac{2\pi}{T_n} = \sqrt{\frac{c}{I_{System}}} \quad \text{Equation 15}$$

Finally, the radius of gyration of the model is given by:

$$k_{xx} = \sqrt{\frac{g(mh + m_F h_F) T_n^2}{4\pi^2 m} - h^2 - \frac{I_F}{m}} \quad \text{Equation 16}$$

3.4.2 Roll Frame

An alternate device to the compound pendulum is the roll frame. This device, shown in Figure 3, is currently used by the National Centre for Maritime Engineering and Hydrodynamics (NCMEH) at the Australian Maritime College in Launceston, Tasmania.



Figure 3 AMC Roll Frame with physical ship model [11].

The roll frame uses a similar approach to the compound pendulum system presented by Lloyd [4] where the model is held in a support frame and is rotated about a pivot point. The period of oscillation of the frame and the frame and model combined are measured by rotating the frame to an initial angle and releasing them. The mass of the model and the righting weight are also measured. The radius of gyration is calculated using the relationship presented in Equation 17.

$$k_{xx} = \sqrt{\frac{g \cdot m_p \cdot h_p (T_2^2 - T_1^2)}{4\pi^2 m_m}} \quad \text{Equation 17}$$

This relationship can be derived from the method proposed by Lloyd [4] for the compound pendulum system as follows. Using the parallel axis theorem, the combined moment of inertia of the frame and model system is represented by Equation 13 and the stiffness of the system is represented by Equation 14. The radius of gyration of the system is represented by Equation 15. Given the frequency of oscillation of the system is:

$$\omega_n = \frac{2\pi}{T_n} = \sqrt{\frac{c}{I_{System}}} \quad \text{Equation 18}$$

The system's moment of inertia is given by:

$$I_{System} = \frac{c}{\omega_n^2} \quad \text{Equation 19}$$

By substituting Equation 14 and Equation 15 into Equation 19 the moment of inertia becomes:

$$I_{System} = \frac{(mh + m_F h_F) \cdot g \cdot T_n^2}{4\pi^2} \quad \text{Equation 20}$$

By substituting Equation 20 into Equation 14 the radius of gyration becomes:

$$k_{xx}^2 = \frac{(mh + m_F h_F) \cdot g \cdot T_n^2}{4\pi^2 m} - h^2 - \frac{I_F}{m} \quad \text{Equation 21}$$

The centre of rotation of the model and frame system is coincident with its centre of mass. Consequently the height term (h) becomes zero and the pendulum mass and distance terms can be substituted for the frame mass and distance terms respectively.

Therefore, Equation 21 becomes:

$$k_{xx}^2 = \frac{(m_P h_P) \cdot g \cdot T_n^2}{4\pi^2 m} - \frac{I_F}{m} \quad \text{Equation 22}$$

Using Equation 22 for the roll frame and the roll frame and model systems independently, we can determine the roll radius of gyration for both systems. By subtracting the solution for the roll frame from the roll frame and model solution, we can determine the roll radius of gyration for the model as shown in Equation 17.

3.4.3 Roll Decay Test

An alternate method to determine the roll gyradius of the model in air is to measure it in water using a calm water roll decay test. The roll gyradius can be directly calculated from the metacentric height and the roll period of the model as determined from the roll decay

test. The metacentric height can be measured by conducting an in-water inclining test prior to the roll decay test. The roll gyradius can be calculated by transposing Equation 1 to become Equation 23 where the average roll period ($T_{\phi Ave}$) of the model can be substituted for roll period (T_{ϕ}).

$$k_{xx}'' = \frac{T_{\phi Ave} \cdot \sqrt{g \cdot GM_T}}{2\pi} \quad \text{Equation 23}$$

The average roll period ($T_{\phi Ave}$) of the model is directly measured from the roll decay trace by identifying the elapsed time for a complete oscillation (peak to peak) as shown in Figure 4. The average period is calculated using the series of measured periods (Equation 24).

$$T_{\phi Ave} = \frac{1}{n} \sum_{i=1}^{i=n} T_i \quad \text{Equation 24}$$

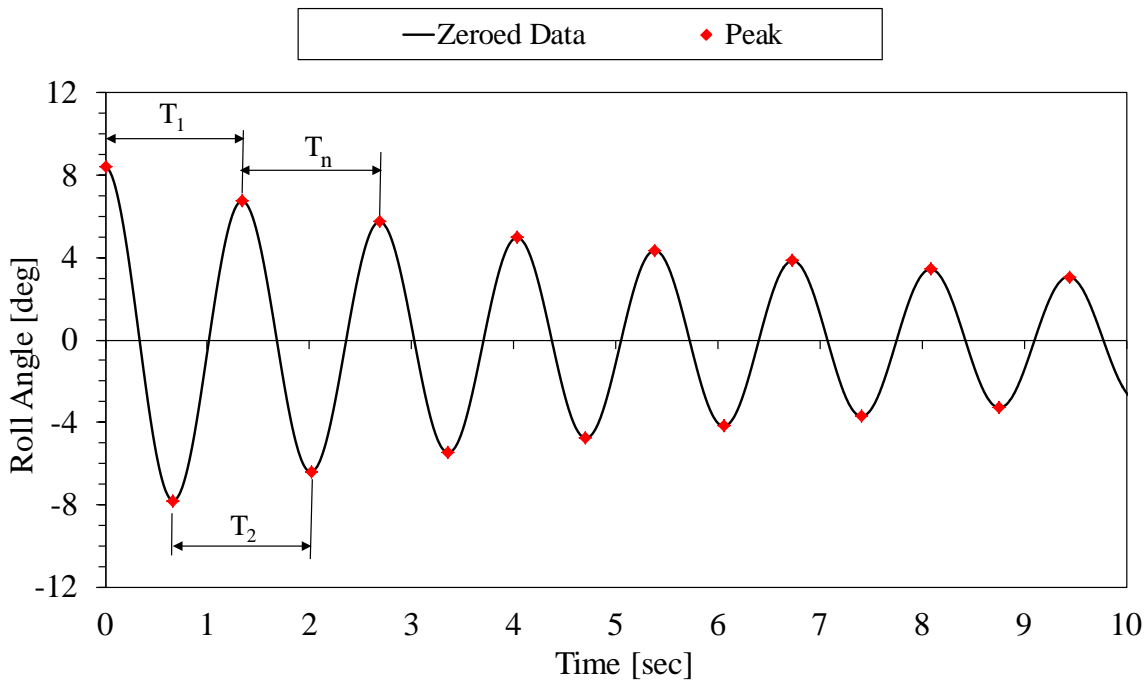


Figure 4 Example roll decay test data: time series roll response indicating the peak to peak measurement of the roll period.

The roll decay motion of the model can be measured experimentally using a range of sensors and set-up configurations. The AMC currently uses the QUALISYS three-dimensional digital video motion capture system installed in its Model Test Basin. The system uses 8 Qqus300 infrared cameras, 16 permanent reference markers and a minimum of 3 model borne marker balls to track the three rotational and three translational motions of the model. The AMC QUALISYS system possesses a linear displacement measurement accuracy of ± 0.25 millimetres and an angular displacement measurement accuracy of \pm

0.05 degrees over a linear marker separation distance of 1000 millimetres. The advantage of using a non-contact test system like QUALYSIS is that it does not introduce external sources of damping into the model's dynamic system.

3.5 Summary

The prominent and applicable methods to determine the added mass and roll gyradius of physical or virtual platform models have been identified and discussed. Each of the methods described has advantages and disadvantages in the context of applicability (to platform type and operating condition), operability (ease of operation), resource requirements (operating costs and schedule) and accuracy of results. As previously mentioned, the accuracy and the applicability of roll gyradius test results have a significant influence on numerical ship motion simulation and analysis. Consequently, further analysis and discussion of the accuracy of the methods used to determine roll gyradius are presented in the following sections.

4. Sensitivity Studies and Uncertainty Analyses

This section presents the results of the sensitivity and uncertainty analyses completed to investigate and identify the critical parameters of the physical test methods used by DSTO and the AMC and provide a quantitative indication of the uncertainty in each measurement method. The methods analysed are:

1. Determining roll gyradius using the roll frame
2. Determining metacentric height using an inclining experiment
3. Measuring the roll period and subsequently determining the roll gyradius using a free roll decay test.

4.1 Sensitivity Study

A local sensitivity analysis of the methods to measure the metacentric height and roll gyradius was completed to investigate the effect of error in each measured input parameter on the error in the output parameter. This was done using the OFAT (one factor at a time) approach. In each instance, the OFAT method is completed by varying one input parameter while holding the remaining input parameters fixed and observing the effect on the output parameter. In each of the three cases investigated the input parameters were varied across a range from -5% to +5%.

The initial input parameter values used as the nominal (baseline) condition were sourced from a set of experiments conducted by DSTO in 2011. The test data relates to a generic landing craft hull form (model AMC-97-07 shown in Figure 5) that was ballasted in a 'heavy' load condition. The target displacement and hydrostatic parameters for the model in the heavy condition were:

$$\begin{aligned}\Delta &= 54.510 \text{ kg} \\ k_{xx} &= 0.125 \text{ m (in air)} \\ KG &= 0.135 \text{ m} \\ GM_T &= 0.039 \text{ m (} KM_T = 0.174 \text{ m at this load condition)}\end{aligned}$$



Figure 5 Generic landing craft model AMC-97-07.

4.1.1 Roll Frame: Roll Gyradius

The formulation of roll gyradius with respect to the roll frame test parameters is represented by Equation 17. It is repeated below for convenience.

$$k_{xx} = \sqrt{\frac{g \cdot m_p \cdot h_p (T_2^2 - T_1^2)}{4\pi^2 m_m}}$$

The following initial input parameters were recorded during the test conducted by DSTO at the AMC in 2011:

$$\begin{aligned} m_p &= 2.584 \text{ kg} \\ h_p &= 0.584 \text{ m} \\ T_1 &= 2.120 \text{ sec} \\ T_2 &= 2.595 \text{ sec} \\ m_m &= 54.510 \text{ kg} \end{aligned}$$

The result of the roll frame roll gyradius sensitivity study shown in Figure 6 indicates that the measurement error in the oscillation times (T_1 and T_2) are the most significant contributor to the error in the measurement of k_{xx} . In addition to this, as T_1 and T_2 tend towards each other ($T_1 \approx T_2$), the change in output parameter increases significantly for the same range of change in input parameter. As T_1 and T_2 tend away from each other ($T_1 \ll T_2$) the change in output parameter reduces and tends towards the change in output parameter for the combined change in T_1 and T_2 , where the change in input and output is directly proportional.

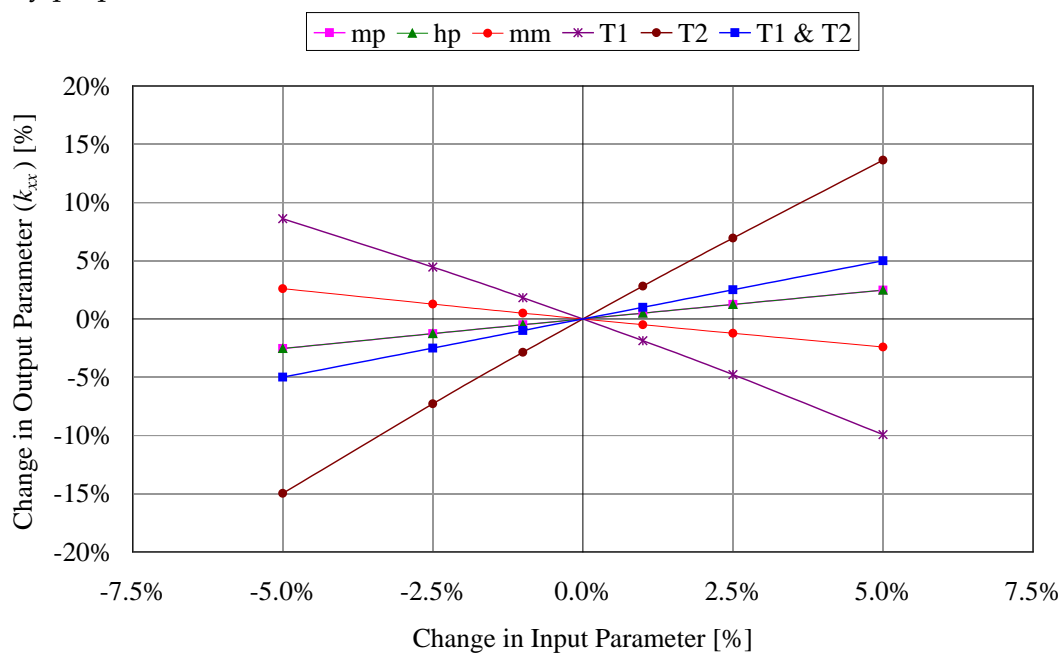


Figure 6 OFAT sensitivity study results for the roll frame method of determining the platform's roll gyradius.

It can be concluded that, of the measured input parameters, it is important to minimise the measurement error in the oscillation times, but also to ensure that the period of oscillation of the frame and model (T_2) is significantly greater than the frame alone (T_1). This behaviour is also apparent in the asymmetric and non-linear response of the T_1 and T_2 curves. Considering the baseline input values used in this analysis, and neglecting the actual oscillation period measurement errors, it would appear that the periods of oscillation are unfavourably close in magnitude as Figure 6 shows that the change in output is large compared to the change in input.

The obvious means to increase the difference between the natural periods of oscillation of the frame and frame with model configurations are to increase the period of the frame with model (T_2) and/or reduce the frame only period (T_1). On inspection of the existing roll frame device it is apparent that there is limited scope to reduce the natural period of oscillation of the frame alone. The only changes that can be implemented, without actual physical modification, are to reduce the pendulum mass (m_p) and the pendulum length (h_p). However, any change in these parameters will be observed, albeit to a lesser extent, in the frame with model condition as the two are not mutually exclusive. Therefore it is more effective to increase the natural period of oscillation of the frame with model configuration. This can be achieved by increasing either the mass of the model (m_m) or the roll gyradius (k_{xx}) or both. Realising a change like this is not readily possible as the mass and roll gyradius of the model are prescribed (fixed) parameters. The only identified alternative to resolve this issue is to match a model and roll frame that will result in significantly different periods of oscillation for the two test conditions. Given the variability in the range of model size, mass and roll gyradius that are likely to be tested, this becomes a complex engineering design problem. Addressing this particular problem is outside of the scope of this investigation.

4.1.2 Inclining Test: Metacentric Height

The method to determine the metacentric height from an inclining test is described by Equation 25. As discussed by Lewis [12], the inclining test method is appropriate for maximum angles of incline (θ) of ± 2 degrees.

$$GM_T = \frac{m \cdot d}{M \cdot \tan \theta} \quad \text{Equation 25}$$

The following initial input parameters were recorded during the test conducted by DSTO at the AMC in 2011:

$$\begin{aligned} m &= 0.260 \text{ kg} \\ d &= 0.174 \text{ m} \\ \Delta &= 54.510 \text{ kg} \\ M &= (\Delta + m) = 54.770 \text{ kg} \\ \theta &= 1.112 \text{ deg} \end{aligned}$$

The result of the inclining experiment GM_T sensitivity study shown in Figure 7 indicates that the influence of the measurement error in each of the input parameters is approximately equal, albeit with no consideration of the direction of their proportionality. The sensitivity of the output parameter is independent of any change in the order of

magnitude of its input parameters. That is, for example, when the inclining mass (m) was changed from 0.260 kg to 2.600 kg or 26.000 kg there was no change in the relationship between percentage change in input and output parameter. This behaviour was observed for each of the input parameters.

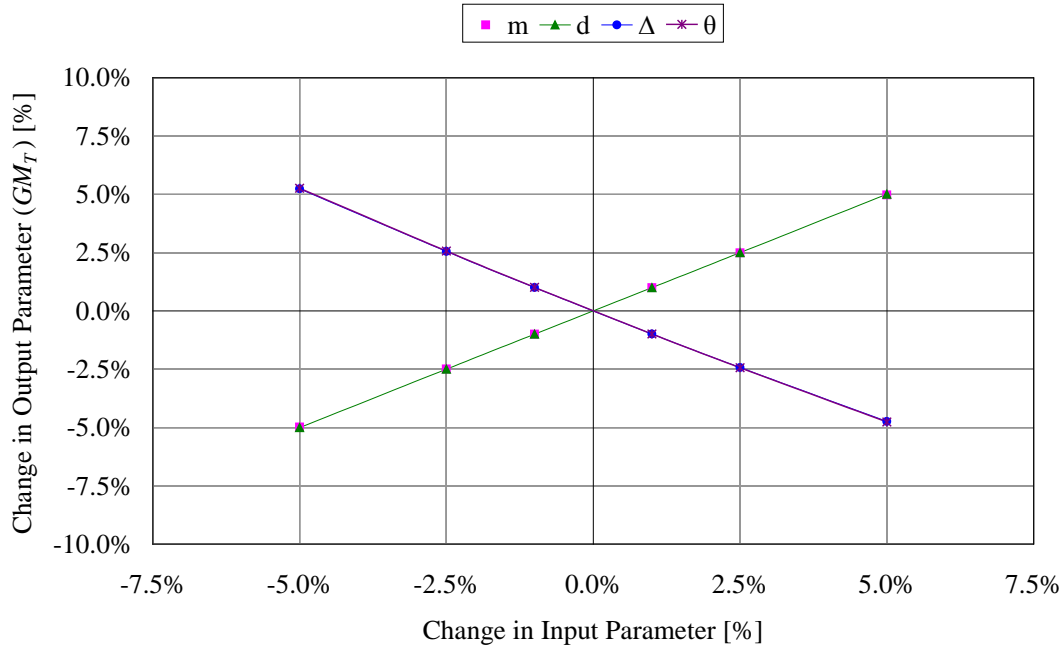


Figure 7 OFAT sensitivity study results for the inclining test method of determining the platform's metacentric height.

4.1.3 Roll Decay Test: Roll Gyradius

The formulation of roll gyradius with respect to the roll frame test parameters is represented by Equation 23. It is repeated below for convenience.

$$k''_{xx} = T_{\phi Ave} \frac{\sqrt{g \cdot GM_T}}{2\pi}$$

The following initial input parameters were recorded during the test conducted by DSTO at the AMC in 2011:

$$T_{\phi Ave} = 1.061 \text{ sec}$$

$$GM_T = 0.042 \text{ m}$$

The result of the roll decay roll gyradius (k''_{xx}) sensitivity study shown in Figure 8 indicates that the influence of the measurement error in the roll period ($T_{\phi Ave}$) is the dominant source of uncertainty in the output parameter. In comparison, the metacentric height has only half the influence of the roll period. Considering that matching an experimentally measured and numerically predicted roll response is of significant value to ship motion analyses, it is apparent that it is more important to minimise the error in the

roll period input parameter. The sensitivity of the output parameter is independent of any change in the order of magnitude of the input parameters.

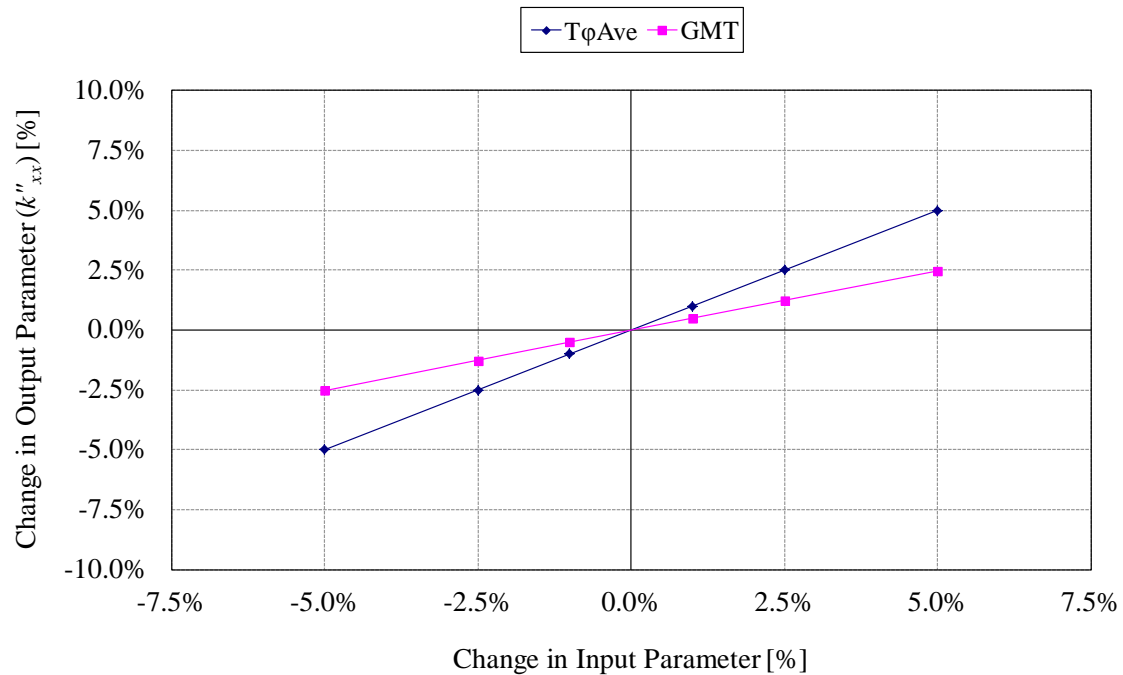


Figure 8 OFAT sensitivity study results for the method of determining the platform's roll gyradius using a roll decay test.

4.2 General Uncertainty Analyses

A general uncertainty analysis was completed to investigate the proportion of the uncertainty in each of the measurement methods for the same model and load condition used in the sensitivity study. In each instance the data reduction equation has been analysed using an error propagation approach to evaluate the uncertainty in the experimental result. The general uncertainty analysis methodology used in this analysis follows the method presented by Coleman and Steele [13]. All uncertainty estimates are quoted at a 95% confidence level. The detailed derivation of the error propagation partial differential equations are presented in Annex C.

4.2.1 Roll Frame Test: Roll Gyradius (in air)

The data reduction equation used to determine the roll gyradius is defined by Equation 17. The resulting error propagation equation used to determine the uncertainty in the roll gyradius (k_{xx}) is:

$$\left(\frac{U_{k_{xx}}}{k_{xx}}\right)^2 = \left(\frac{U_{m_p}}{2m_p}\right)^2 + \left(\frac{U_{h_p}}{2h_p}\right)^2 + \left(\frac{(T_2^2 - 2T_1) \cdot U_{T_1}}{2(T_2^2 - T_1^2)}\right)^2 + \left(\frac{(2T_2 - T_1^2) \cdot U_{T_2}}{2(T_2^2 - T_1^2)}\right)^2 + \left(-\frac{U_{m_m}}{2m_m}\right)^2$$

Equation 26

The following uncertainty estimates were recorded during the test conducted by DSTO at the AMC in 2011:

$$\begin{aligned} U_{m_p} &= 0.001 \text{ kg} \\ U_{h_p} &= 0.002 \text{ m} \\ U_{T_1} &= 0.050 \text{ sec} \\ U_{T_2} &= 0.050 \text{ sec} \\ U_{m_m} &= 0.001 \text{ kg} \end{aligned}$$

For AMC-97-07 (2011):

$$\begin{aligned} m_p &= 2.584 \text{ kg} \\ h_p &= 0.584 \text{ m} \\ T_1 &= 2.120 \text{ sec} \\ T_2 &= 2.595 \text{ sec} \\ m_m &= 54.510 \text{ kg} \end{aligned}$$

Using the uncertainty estimates that were determined based on the measurement equipment used in the test and the measured test parameters for the model (AMC-97-07), the calculated roll gyradius and its measurement uncertainty is calculated as follows:

$$\left(\frac{U_{k_{xx}}}{k_{xx}}\right)^2 = \left(\frac{0.001}{2(2.584)}\right)^2 + \left(\frac{0.002}{2(0.584)}\right)^2 + \left(\frac{(2.595^2 - 2(2.120)) \cdot 0.05}{2(2.595^2 - 2.120^2)}\right)^2 + \left(\frac{(2(2.595) - 2.120^2) \cdot 0.05}{2(2.595^2 - 2.120^2)}\right)^2 + \left(-\frac{0.001}{2(54.510)}\right)^2$$

Equation 27

$$\frac{U_{k_{xx}}}{k_{xx}} = 0.029 = 2.90\%$$

Equation 28

$$k_{xx} = 0.122 \pm 0.003m$$

Equation 29

4.2.2 Inclining Test: Metacentric Height

The data reduction equation used to determine the metacentric height (GM_T) is defined by Equation 25. The resulting error propagation equation used to determine the uncertainty in the metacentric height (GM_T) is:

$$\left(\frac{U_{GM_T}}{GM_T}\right)^2 = \left(\frac{U_m}{m}\right)^2 + \left(\frac{U_d}{d}\right)^2 + \left(-\frac{U_M}{M}\right)^2 + \left(-\frac{\tan \theta \cdot U_\theta}{(1 + \tan^2 \theta)^2}\right)^2 \quad \text{Equation 30}$$

The following uncertainty estimates were recorded during the test conducted by DSTO at the AMC in 2011:

$$\begin{aligned} U_m &= 0.001 \text{ kg} \\ U_d &= 0.002 \text{ m} \\ U_M &= 0.001 \text{ kg} \\ U_\theta &= 0.100 \text{ deg} = 1.745\text{E-}3 \text{ rad} \end{aligned}$$

For AMC-97-07 Run 85 (2011):

$$\begin{aligned} m &= 0.260 \text{ kg} \\ d &= 0.174 \text{ m} \\ M &= 54.770 \text{ kg} \\ \theta &= 1.112 \text{ deg} = 1.940\text{E-}2 \text{ rad} \end{aligned}$$

Using the uncertainty estimates that were determined based on the measurement equipment used in the test and the measured test parameters for the model (AMC-97-07), the calculated metacentric height and its measurement uncertainty is calculated as follows:

$$\begin{aligned} \left(\frac{U_{GM_T}}{GM_T}\right)^2 &= \left(\frac{0.001}{0.260}\right)^2 + \left(\frac{0.002}{0.174}\right)^2 + \left(-\frac{0.001}{54.770}\right)^2 \\ &+ \left(-\frac{\tan(1.940\text{E-}2) \cdot 1.745\text{E-}3}{(1 + \tan^2(1.940\text{E-}2))^2}\right)^2 \end{aligned} \quad \text{Equation 31}$$

$$\frac{U_{GM_T}}{GM_T} = 0.0121 = 1.21\% \quad \text{Equation 32}$$

$$GM_T = 0.042 \pm 0.001\text{m} \quad \text{Equation 33}$$

4.2.3 Roll Decay Test: Roll Gyradius (in water)

The data reduction equation used to determine the roll gyradius in water (k''_{xx}) is defined by Equation 23. The resulting error propagation equation used to determine the uncertainty in the roll gyradius (k''_{xx}) is:

$$\left(\frac{U_{k''_{xx}}}{k''_{xx}}\right)^2 = \left(\frac{U_{T_\phi}}{T_\phi}\right)^2 + \left(\frac{U_{GM_T}}{GM_T}\right)^2 \quad \text{Equation 34}$$

The following uncertainty estimates were recorded during the test conducted by DSTO at the AMC in 2011:

$$U_{T_\phi} = 0.020 \text{ sec}$$

$$U_{GMT}/GM_T = 1.21\%$$

For AMC-97-07 Run 86 (2011):

$$T_{\phi Ave} = 1.480 \text{ sec}$$

$$GM_T = 0.042 \text{ m}$$

Using the uncertainty estimates that were determined based on the measurement equipment used in the test, the uncertainty estimate of the metacentric height determined from the inclining experiment and the measured test parameters for the model (AMC-97-07) the calculated roll gyradius (in water) and its measurement uncertainty is calculated as follows:

$$\left(\frac{U_{k_{xx}''}}{k_{xx}''} \right)^2 = \left(\frac{(0.020)}{1.480} \right)^2 + (0.0121)^2 \quad \text{Equation 35}$$

$$\frac{U_{k_{xx}''}}{k_{xx}''} = 0.018 = 1.81\% \quad \text{Equation 36}$$

$$k_{xx}'' = 0.184 \pm 0.003m \quad \text{Equation 37}$$

4.3 Discrete Element Method: Discretization Sensitivity Analysis

A sensitivity analysis was completed to investigate the effect of object discretization on the gyradius calculated using the discrete element method. A square panel with an edge length of one metre and a thickness of ten millimetres was used as the test object. The panel was discretized into equal sized elements by dividing its perimeter edges by a factor of 2, 4, 8 and 16 to form four different test samples (Figure 9).

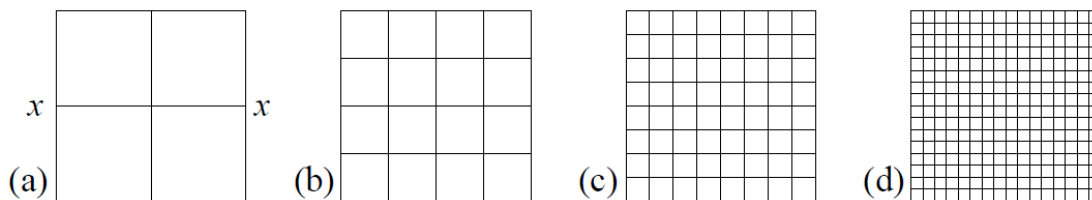


Figure 9 Discretized 1m x 1m x 0.01m square panel: (a) $n = 4$ elements (b) $n = 16$ elements (c) $n = 64$ elements (d) $n = 256$ elements.

The discrete element method (Equation 10) was used to calculate the panel's radius of gyration about its x - x axis using the four different discretized geometries. The calculated

result was compared against the analytical solution presented in Equation 38 where 'a' is the edge length of the panel.

$$k_{xx} = \sqrt{\frac{1}{12}} \cdot a \quad \text{Equation 38}$$

The results of the comparison indicate that the relative error between the calculated result and the analytical result decreases with a power function as the level of discretization is increased (Figure 10). For the uniform square geometry it was calculated that a minimum of 50 elements are required to achieve a relative error of one percent. Based on this result, it is apparent that the application of the method to a highly detailed and complex ship geometry is prohibitive in the context of accuracy and efficiency. On reflection, the CAD method described in § 3.3 represents an efficient embodiment of the discrete element method and a more effective alternative to determining the roll gyradius of a virtual ship geometry.

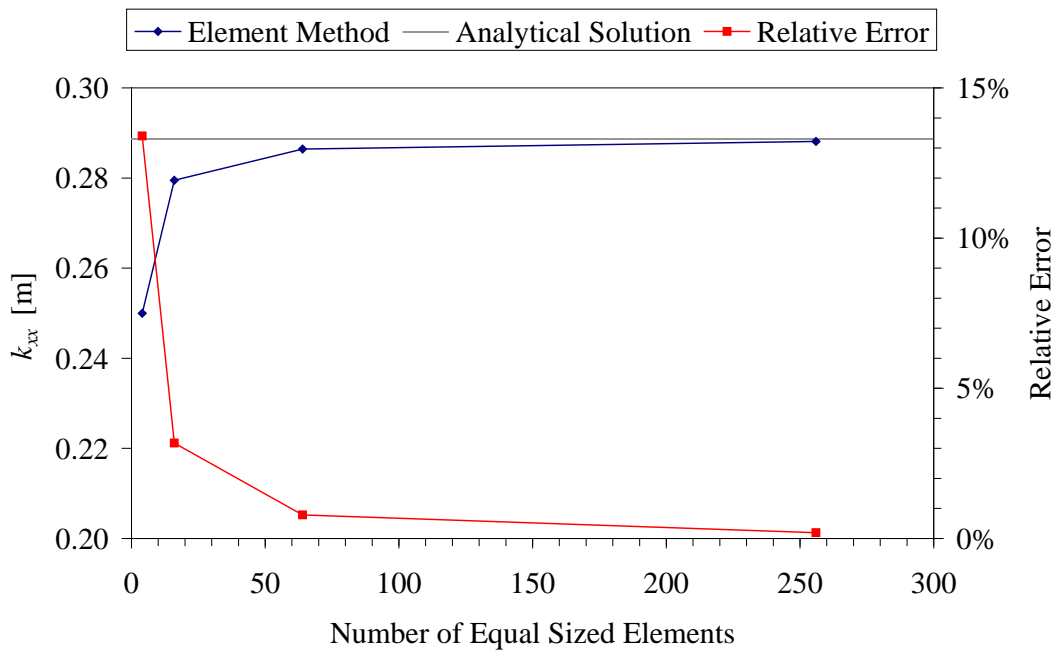


Figure 10 Discretization sensitivity analysis of the element method: Element method compared to analytical solution of the gyradius of a 1m x 1m x 0.01m panel.

4.4 Summary

The results of the sensitivity and uncertainty analyses indicate the following:

1. When using a roll frame device to determine the roll gyradius of a physical model it is important to minimise the error in the measurement of the time of oscillation as this has the greatest influence on the error of the calculated result.
2. It is important to use a roll frame which has a period of oscillation that is significantly less than that of the model and roll frame combined. If the period of oscillation of the

frame only and model with frame configurations are too similar the influence of an error in the time measurement on the calculated result increases significantly.

3. For the landing craft model and load condition used in the preceding analyses to determine its roll gyradius, it is apparent that there is a lower uncertainty in the calculated result using the roll decay test method when compared to the roll frame method.
4. For the landing craft model and load condition used in these analyses to determine the metacentric height using an inclining experiment, the uncertainty in the measurement is low (1.21%) and this measurement method is considered to be acceptable if conducted in accordance with the principles presented by Lewis [14] and using the AMC QUALYSIS system and operating procedures.
5. Based on the simple geometry analysed to evaluate the performance of the element method and the results of the analysis, this method has been found to be an inefficient and ineffective way of determining the roll gyradius of the complex geometries typical of maritime platforms.

5. Solutions

In addressing the fundamental issues experienced by Hill et al. [1], two forms of solution have been identified: the requirement to change existing programmatic (planning, test and analysis) procedures and processes; and the synthesis of existing test methods to form functional, system level solutions. Together these two forms of solution represent the holistic solution to the issues encountered by Hill et al. [1] and a qualified and traceable method to be used in future test programs.

5.1 Procedural Guidance

Two forms of procedural guidance have been developed in conjunction with the system level solutions presented in § 5.2 to address the issues identified at the start of this investigation. The two issues addressed by the procedural guidance are:

1. The ambiguities in the specification of the required test roll gyradius.
2. The lack of an explicit statement of guidance to direct the experimenter/analyst to the appropriate method for determining the roll gyradius of their platform with respect to their intended analyses.

In addressing the first issue it is proposed that the specification of the roll gyradius requirement for a maritime platform, whether model scale or full scale, should be structured using the following formats.

When assigning a roll gyradius to a model or full scale platform, whether physical or virtual, the following statement should be tailored and used:

The roll gyradius of the [platform identifier] in the [load condition descriptor] load condition shall be equal to [quantitative value of the roll gyradius] metres ±[required accuracy] metres. The roll gyradius is that of the [platform identifier] when measured in a [descriptor of the medium in which the roll gyradius is measured: in-water or out of water] condition and therefore [includes/does not include] the effects of hydrodynamic added mass. In instances where an in-water roll gyradius is required, the assigned roll gyradius corresponds to that of the platform floating in a deep water condition.

When reporting on the measurement, computation or calculation of a platform's roll gyradius the following statement should be tailored and included in the report or data document:

The roll gyradius of [platform identifier] in the [load condition descriptor] load condition has been determined to be [quantitative value of the roll gyradius] metres ±[include uncertainty estimate] metres. The roll gyradius was determined using the [measurement method descriptor] method and represents the platform when in a [dry, out of water/ in water] condition.

In addressing the second issue, a process flowchart (Decision Tree) has been developed to provide guidance to the analyst/experimenter as to which of the proposed system level solutions, presented in § 5.2, should be employed to determine the roll gyradius of a platform. The platform may be either a physical scale model (commonly used for scale model experiments in a hydrodynamic test facility) or a virtual model. The virtual model may be of a conceptual platform design, a computer prototype of a physical scale model (used for the purpose of experiment design), or an existing full scale platform. The Decision Tree is presented in Appendix A.

The activities captured in the Decision Tree assume that the experimenter/analyst is capable of conducting each activity or at least has access to resources that can provide the data output from the activities. Following the Decision Tree does not assure the quality of the outcomes of each activity nor the data used as inputs to the activities.

5.2 System Level Solutions

Three system level solutions have been identified based on the theoretical formulation of roll gyradius and added mass presented in § 2, the available methods of determining these two parameters discussed in § 3 and the quantitative evaluation of the performance of these methods presented in § 4. The solutions address the following investigation objectives presented in § 1:

1. Establish an experimental approach to measure the roll gyradius of a physical model in calm water.
2. Establish a method for predicting the roll gyradius, and hence roll period, for a physical model (and full scale ship) without need for experiment.

The system level solutions are:

1. Conduct an in-water inclining test and roll decay test for the model in its ballast condition.
2. Conduct an in-air oscillation test using a roll frame device to determine the model's in-air roll gyradius. The roll frame has been chosen in preference to the pendulum method due to its portability and ease of operation. A correction for the in-water roll gyradius is required and can be achieved by using a numerical approach to calculate the roll added mass component at the natural roll frequency.
3. Computer modelling: Use of a CAD solid modelling program to model the physical geometry and calculate its principal gyradii (including the roll gyradius). A correction for the in-water roll gyradius is required and can be achieved by using a numerical approach to calculate the roll added mass component at the natural roll frequency. Where a detailed CAD solid model is not available, or the effort to generate one is too great, this data may be replaced by the platform's mass distribution data or a roll gyradius determined empirically and based on the platform type and load condition.

The identified resource requirements, advantages and disadvantages of each of these solution options have been collated and are presented in Table 1. When selecting one of the proposed solutions, the analyst should give consideration to the operational requirements and constraints that are unique to its application.

Table 1 Resource requirements, advantages and disadvantages of roll gyradius measurement and prediction methods.

Method	Resource Requirements	Advantages	Disadvantages
1. In-Water Roll Decay Test	Physical model Model in ballasted condition Model hydrostatic data Test facility Motion measurement, data acquisition and post-processing system	Directly applicable to scale models. This method allows the experimenter to assign the required model ballast condition (KG and k_{xx}) and conduct seakeeping tests immediately. No CAD platform modelling or added mass computations are required.	The test requires the use of a facility of adequate size to accommodate the model and provide clearance to mitigate interference from reflected waves from all rigid boundaries (tank walls). This method provides an output that is targeted at conducting subsequent model tests.
2. Roll Frame Measurement and Added Mass Calculation	Physical model Model in ballasted condition Roll frame device Motion measurement, data acquisition and post-processing system Hull geometry in CAD format (surface model) Added mass calculation capable software	The measurement can be conducted independent of a test facility (test basin or towing tank facility time is not required). The model is directly and easily accessible. This enables timely and accurate modification to the ballast condition.	Additional information and effort is required to determine the added mass component that will act on the platform. A CAD and added mass or ship motion prediction program are required. The analyst must model the physical platform in each load condition in order to predict the corresponding added mass component.
3. CAD Modelling Calculation & Added Mass Calculation	Hull geometry in CAD format (surface and solid model) Load condition data Added mass calculation capable software Supplementary data: <ul style="list-style-type: none"> detailed mass distribution reported or measured roll period and associated load condition when period was recorded 	Suitable for furnishing the simulation requirements of any platform of any scale. No physical model or measurement activity is required. Modifications to model geometry and load condition can be completed quickly. Various load conditions can be calculated and analysed with minimal effort. This method can be used for prototyping and/or designing experimental models.	Detailed mass distribution data is required for the lightship condition to determine the actual roll gyradius of the platform. However, a representative roll gyradius value can be used in way of this calculation. Some additional work is required to determine the added mass component that will act on the platform.

6. Concluding Remarks

When conducting numerical ship motion simulation and analysis it is important to ensure that the simulation input data is accurate and correct. Incorrect data or data used incorrectly will result in erroneous and misleading simulation results. The disparity in roll frequency observed by Hill et al. [1] in their experimental and numerical analysis of landing craft roll motion has led to further investigation to identify the causes of their results. Based on the outcomes of the current investigation it can be concluded that the root cause of the issue experienced by Hill et al. [1] was the incorrect application of their measured roll gyradius data. The discrepancy observed in their results is predominantly due to the absence of the influence of added mass. Nonetheless, this issue prompted further investigation into the process, procedures and equipment used to determine the parameters that influence the roll motion of a platform: the roll radius of gyration and the transverse metacentric height.

The solution to the issues identified throughout this investigation comprise: the introduction/establishment of a requirements statement approach to unambiguously defining the data need; the formulation of a Decision Tree type guidance tool for the experimenter/analyst; and three technology/process based system level methods for determining the roll gyradius of a platform.

Furthermore, the results of these investigations have shown that of the prominent methods to physically measure the roll gyradius of a scale model, the in-water roll decay test is the most effective and accurate. The in-water roll decay test method provides a roll gyradius value that includes the effects of hydrodynamic mass, possess low measurement uncertainty and results in the model being ballasted and prepared for the actual hydrodynamics test program. Notwithstanding this outcome, the roll frame device is also capable of providing an accurate roll gyradius measurement, albeit without the effects of added mass. The roll frame method is a suitable alternative to conducting an in-water test which requires more resources to be allocated. An evaluation of the function and performance of the existing AMC roll frames has indicated that there are limitations associated with the structural integrity of the dynamic frame that may result in increased measurement error under specific testing conditions. This issue is more pertinent to the large roll frame currently operated by the AMC. Further analysis and design modification is required to resolve the issues associated with the current roll frames; however, this is outside of the scope of this investigation. The method of conducting an in-water inclining experiment to determine a model's transverse metacentric height and location of its vertical centre of gravity has also been found to produce an accurate result with acceptable measurement uncertainty. The most effective alternative to physically measuring the roll gyradius of a platform is to use a coupled computational approach. In this case, the in-air roll gyradius of a platform of any size can be determined using three-dimensional solid modelling CAD software. The in-water roll gyradius can then be determined by computing the hydrodynamic added mass using a strip theory based software program.

7. Acknowledgements

The author wishes to thank the following people for their assistance while conducting this investigation: Ms Teresa Magoga for her assistance in using Maestro to conduct the structural analysis of the roll frames; Mrs Jenny Hill for her assistance when conducting the roll frame tests; and Mr Shaun Denehey and Mr Kirk Meyer of the AMC for their assistance in setting up the roll frame and the data acquisition system.

8. References

1. Hill, J., et al., *Investigation into the Roll Behaviour of Landing Craft in Deep Water*, in *PACIFIC 2012 International Maritime Conference*. 2012: Sydney, Australia. p. 497-506.
2. Bhattacharyya, R., *Dynamics of Marine Vehicles*. 1978, New York, USA: Wiley.
3. Lewis, E.V., *Principles of Naval Architecture: Motions in Waves and Controllability*. Vol. 3. 1988, Jersey City, USA: Society of Naval Architects and Marine Engineers.
4. Lloyd, A.R.J.M., *Seakeeping: Ship Behaviour in Rough Waves*. 1989, Sussex, England: Ellis Horwood.
5. Rawson, K.J. and E.C. Tupper, *Basic Ship Theory*. 2001, Oxford, England: Butterworth Heinemann.
6. Frank, W. and N. Salvensen, *The Frank Close-Fit Ship-Motion Computer Program*. 1970, Naval Ship Research and Development Center: Washington D.C.
7. MARIN, *FREDYN Version 10.3 Computer Program for the Simulation of a Steered Ship in Extreme Seas and Wind*. 2011, CRNAV, Maritime Research Institute Netherlands.
8. Inglis, R.B. and W.G. Price, *Motions of Ships in Shallow Water*. Transactions RINA, 1980. **122**: p. 269-284.
9. Robert McNeel and Associates, *Rhinoceros NURBS Modelling for Windows*. 2011: Seattle, Washington.
10. Arden, G., *Description of Method for Calculating Mass Properties of Solids* E. Dawson, Editor. 2013, Robert McNeel & Associates: Melbourne. p. 1.
11. Macfarlane, G.J., *Development of Ship Dynamics Demonstration Models*, in *Committee for University Teaching and Staff Development*. 1998: Launceston, Tasmania.
12. Lewis, E., ed. *Principles of Naval Architecture: Stability and Strength*. Vol. I. 1988, Society of Naval Architects and Marine Engineers: New Jersey, USA.
13. Coleman, H.W. and W.G. Steele, *Experimentation and Uncertainty Analysis for Engineers*. 1999, United States of America: John Wiley & Sons.
14. Lewis, E.V., ed. *Principles of Naval Architecture: Stability and Strength*. Vol. 1. 1988, Society of Naval Architects and Marine Engineers: Jersey City, USA.
15. Macfarlane, G., *Roll Frame Error Sources*, J. Hill, E. Dawson, and T. Turner, Editors. 2011, Australian Maritime College: Launceston, Tasmania.
16. Advanced Marine Technology Centre, *MAESTRO 11.0.0*. 2013, DRS Defence Solutions: Stevensville, USA.
17. International Towing Tank Conference. *Recommended Procedures*. 2008 September 2011]; Available from: <http://ittc.sname.org/documents.htm>.
18. Miller, M.P., *An Accurate Method of Measuring the Moments of Inertia of Airplanes*. 1930, National Advisory Committee for Aeronautics: Washington D.C.

Appendix A: Decision Tree: Method to Determine a Platform's Roll Gyradius

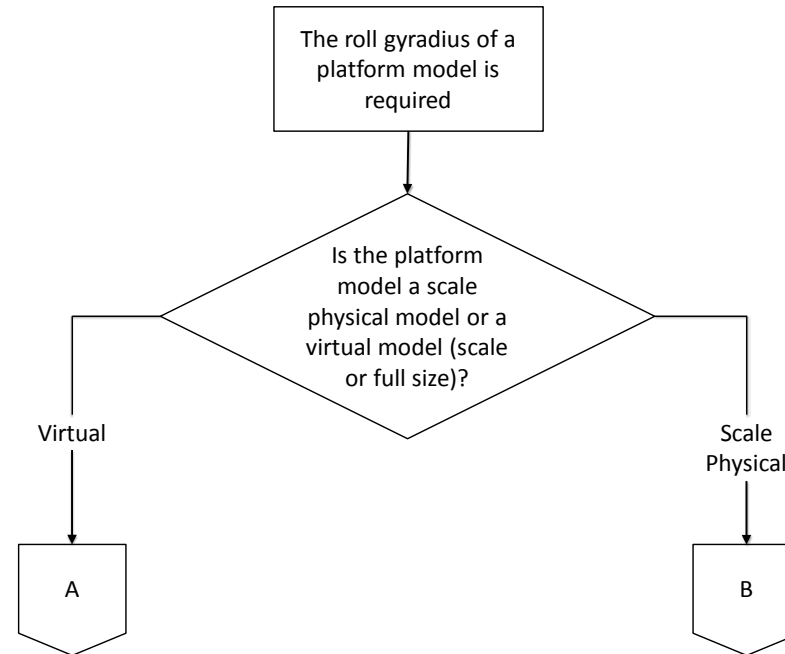


Figure A1 Decision Tree: Start of roll gyradius determination process.

UNCLASSIFIED

DSTO-TN-1402

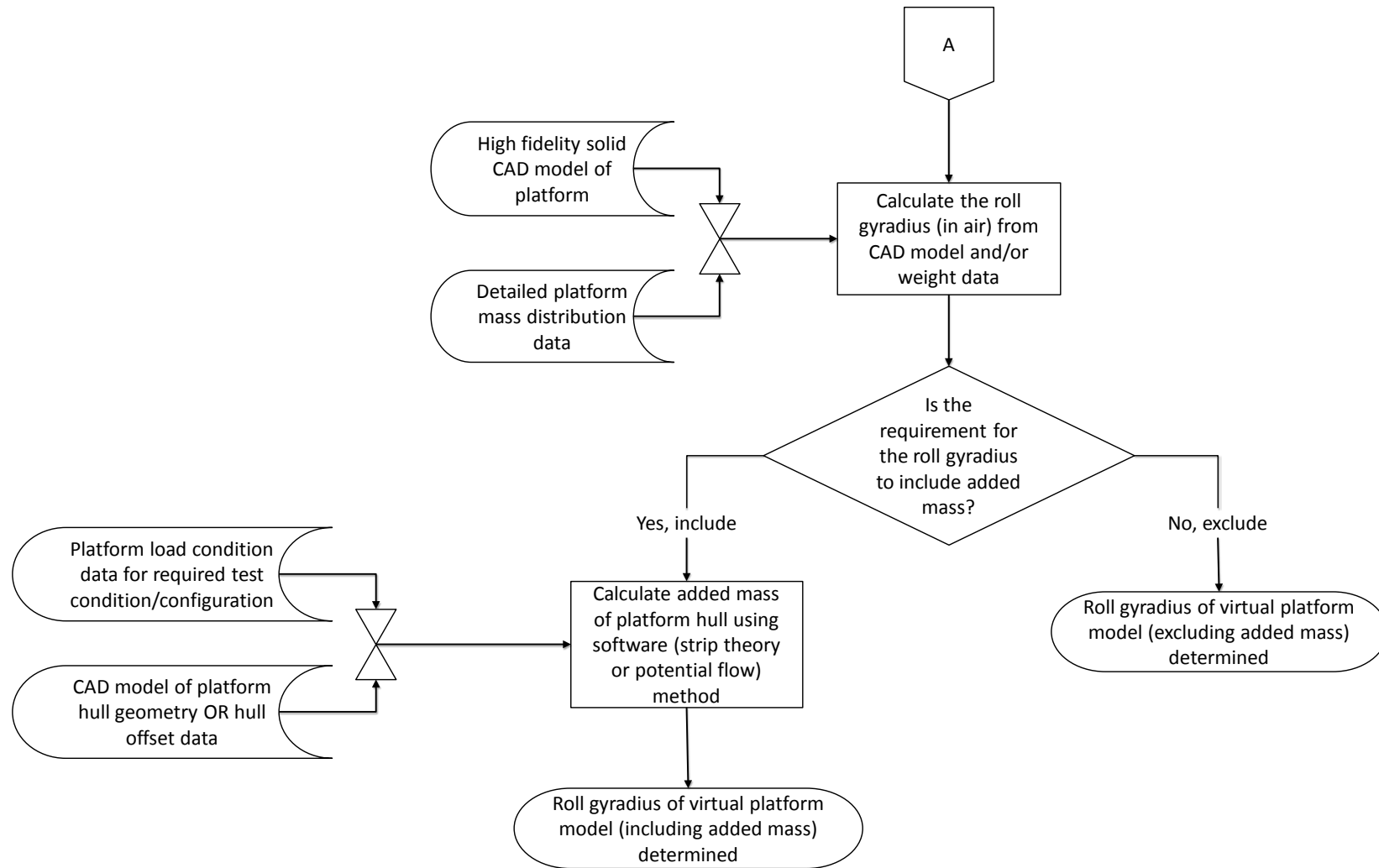


Figure A2 Decision Tree: virtual model decision solution route (virtual model includes a numerical model of a platform that can be either existing or conceptual and of any scale).

UNCLASSIFIED

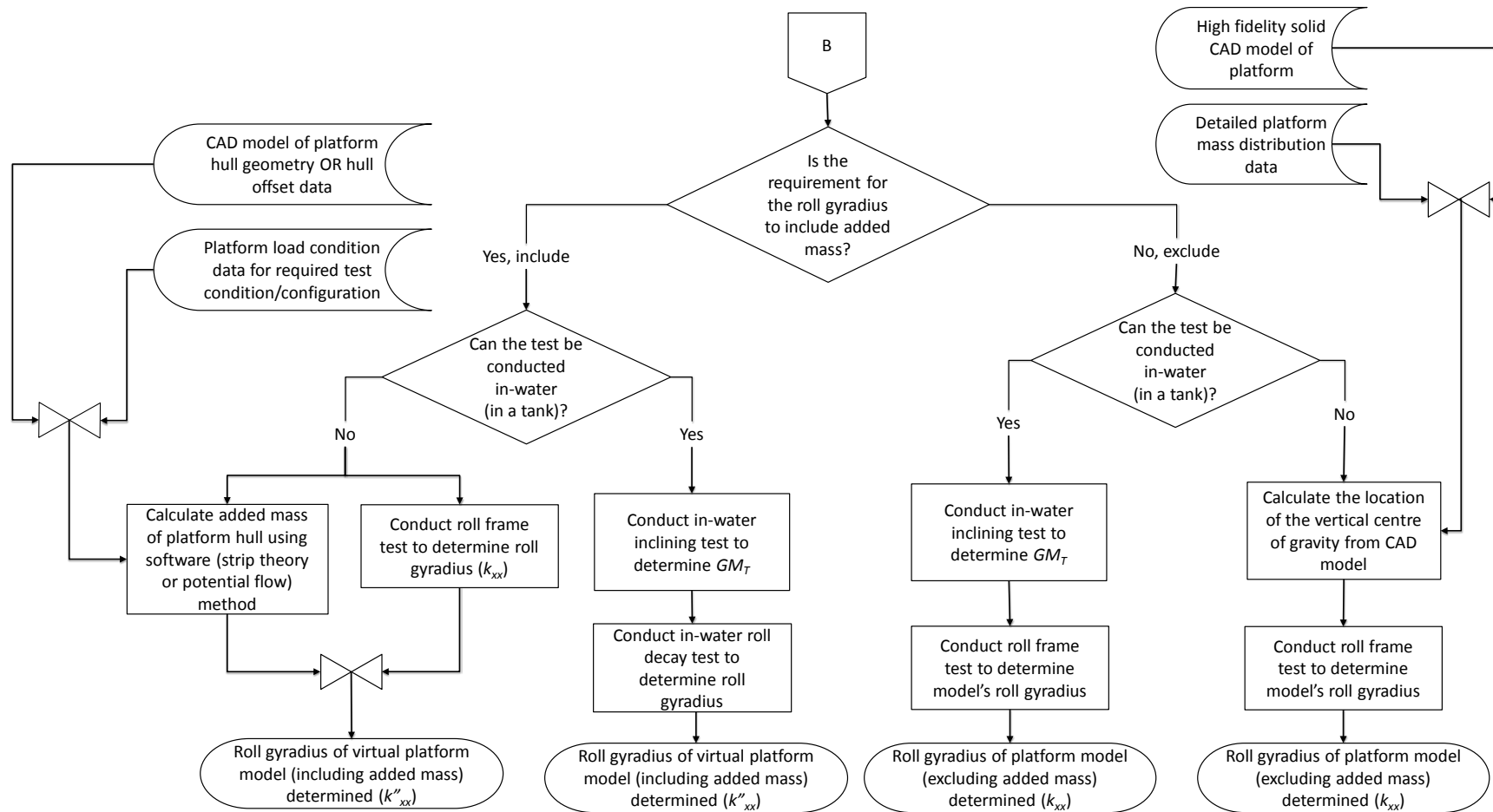


Figure A3 Decision Tree: scale physical model decision solution route.

Appendix B: Roll Frame Function and Performance Evaluation

The function and performance of the small AMC roll frame (Figure B1) were investigated and evaluated by conducting a series of tests to determine the roll radius of gyration of a simple pontoon model (AMC-03-10) and comparing the results to the roll gyradius determined using the CAD method. The objectives of the function and performance evaluation tests were to:

1. Investigate the effects of initial roll angle on the roll gyradius test result.
2. Investigate the effects of the oscillation time measurement system on the roll gyradius test result.
3. Evaluate the user operation procedure and the system function to identify any limitations.

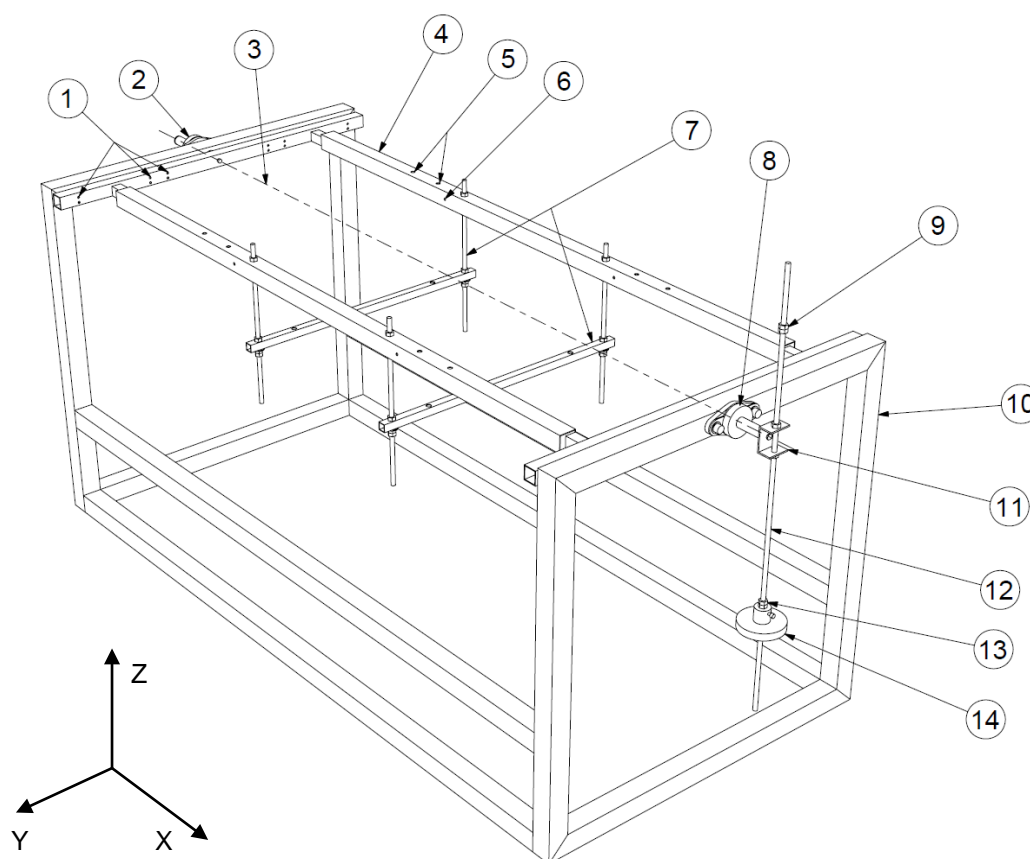


Figure B1 AMC Roll Frame (small). Annotations: 1. Lateral locating points for dynamic frame longitudinal supports (typical); 2. Bearing and shaft arrangement (non-pendulum end); 3. Roll axis; 4. Dynamic frame (assembly); 5. Longitudinal locating points for under-slung supports (typical); 6. Locating hole for lateral securing rods (rods not shown) (typical); 7. Under-slung supports (sub-assembly); 8. Bearing and shaft arrangement (pendulum end); 9. Pendulum weight locating and locking nuts (upper pendulum); 10. Static frame (assembly); 11. Pendulum to dynamic frame interface (sub-assembly); 12. Pendulum arm (threaded rod); 13. Pendulum weight locating and locking nuts (lower pendulum); 14. Pendulum weight.

The small AMC roll frame can be used to determine the roll radius of gyration of models with an overall length of up to 1.65 metres and an overall beam of up to 0.75 metres. There are; however, limitations related to the maximum permissible mass of the model due to the structural integrity of the roll frame. These issues are discussed in § B.3.

B.1. Test Setup, Procedure and Results

The evaluation tests were completed using a simple pontoon model. The model was selected because of its regular and flat sided shape which resulted in a relatively easy setup and measurement process in the roll frame device. Its regular shape and accessible

internal arrangement also made it easy to survey and model the pontoon using the Rhinoceros 3D CAD program. A rendered image of the three dimensional CAD solid model of the pontoon is presented in Figure B2.

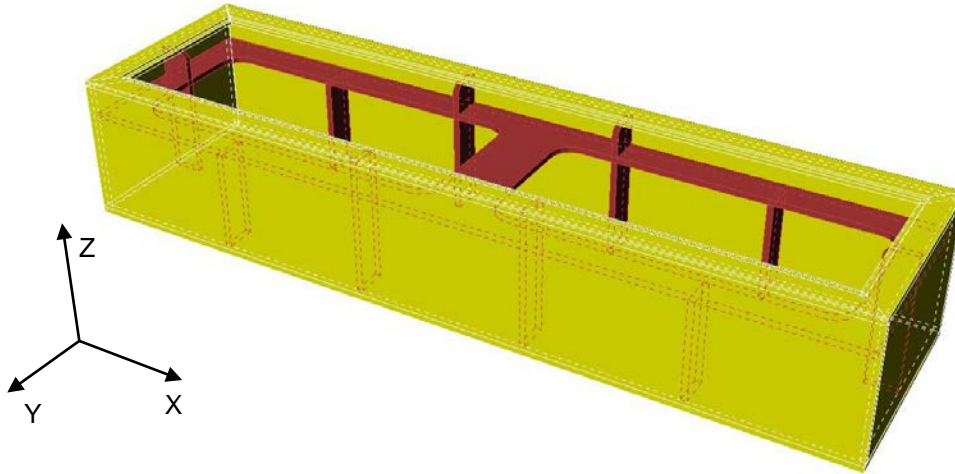


Figure B2 Pontoon model AMC-03-10: overall length = 1.340 m, overall beam = 0.363 m, overall height = 0.250 m, mass in air = 10.649 kg.

The location of the vertical centre of gravity of the model was determined by assuming a homogenous material density and using Rhinoceros 3D to calculate the centre of volume of the three dimensional model. This enabled the model to be aligned to the roll axis of the roll frame during the roll frame test. Two time measurement methods were used. These were the:

1. Two person manual method with each person uses a digital stopwatch (this represents the existing AMC test procedure).
2. Integrated laser encoder and digital data acquisition system.

The integrated laser encoder system architecture is presented in Figure B3. The laser encoder system was configured to record a voltage signal from the encoder at a sampling frequency of 1000 Hz using a PC based National Instruments LabView data acquisition system. A small wooden stave was adhered to the dynamic frame to act as the beam breaker and trigger a spike in the voltage signal (Figure B4). An example of the recorded signal is shown in Figure B5 where each successive pulse in the free oscillation phase represents the stave crossing the laser beam. The time between each pulse equates to half of the natural roll period. It can be observed that as the roll motion decays and the roll amplitude and velocity decrease, the signal pulses develop a flat region at their local minima. This represents the time taken for the width of the stave to pass in front of the laser beam. The period of oscillation was determined by calculating the time differential between the points at which the stave passed the beam when travelling in the same direction. That is, the time differential was calculated between every second pulse and at the same point on the pulse signal: the instant that the pulse occurred.

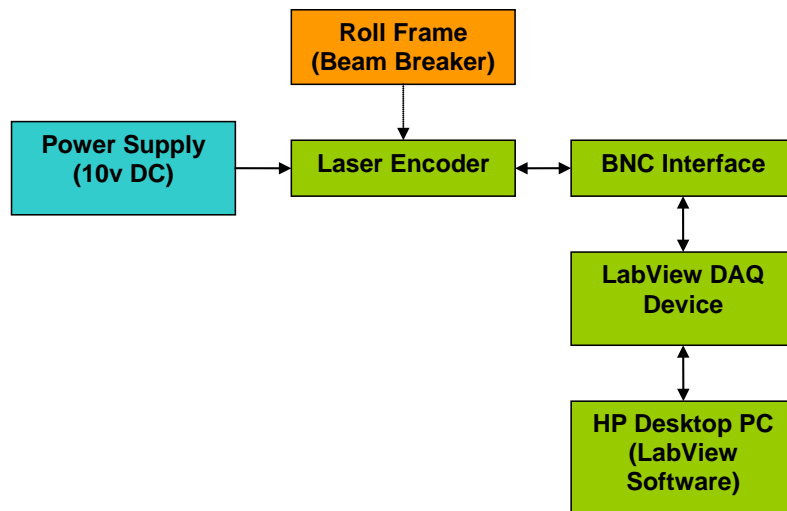


Figure B3 Digital laser encoder time measurement system: system architecture block diagram.

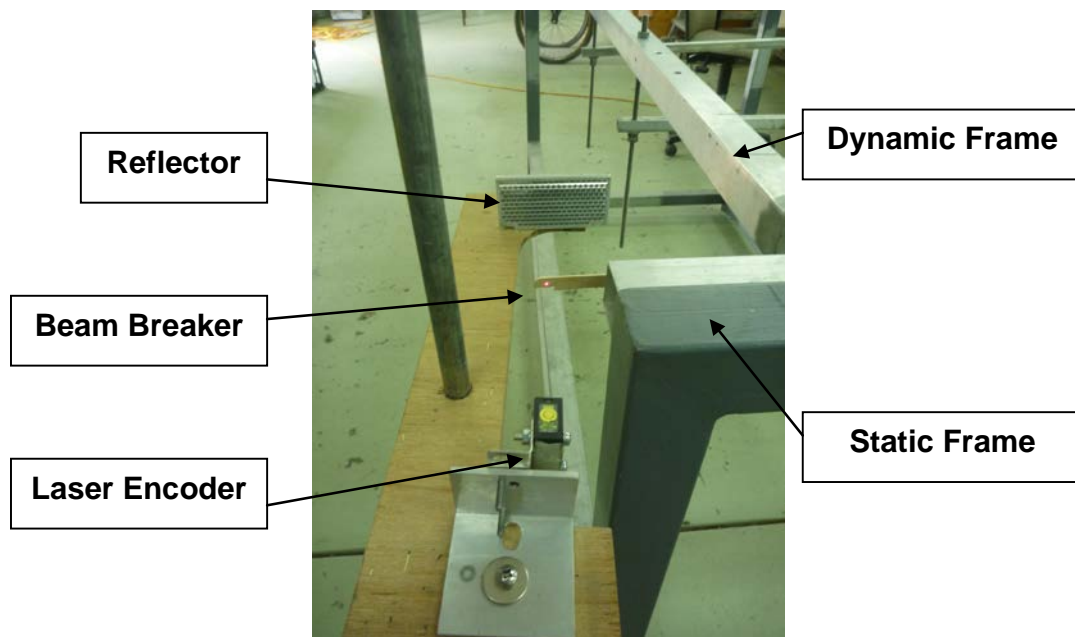


Figure B4 Digital laser encoder time measurement system: physical setup.

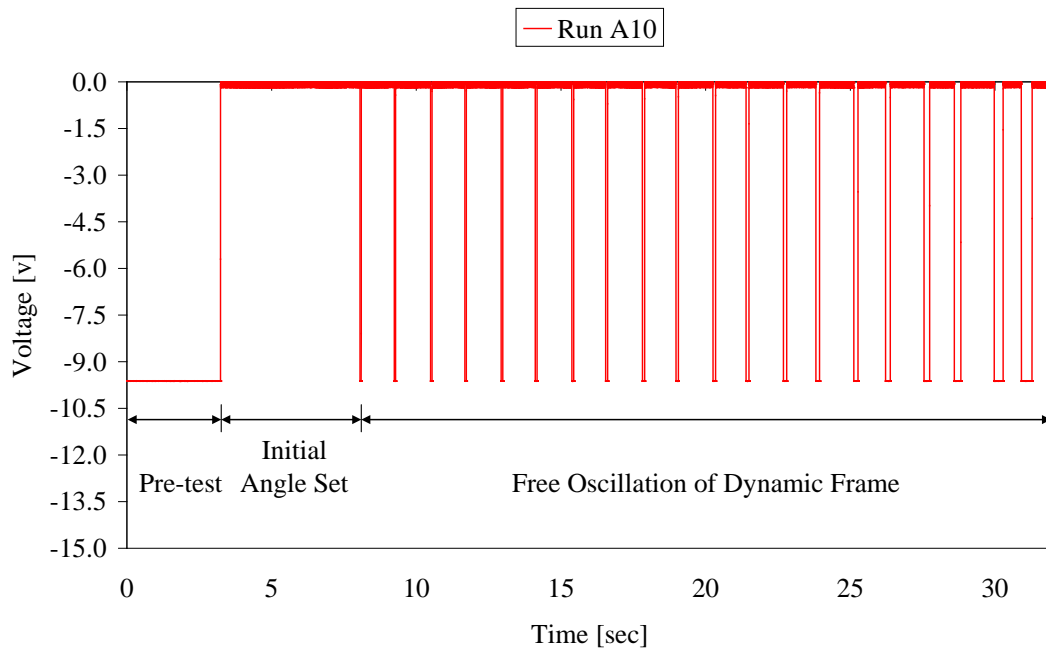


Figure B5 Digital laser encoder time measurement system: recorded voltage signal.

The existing AMC standard operating procedure was executed for the frame setup and test process using the pontoon model. Two operators were used to measure and record the oscillation time using the manual stopwatch method. Ten consecutive oscillations were counted in each of the tests. The laser encoder system was operated simultaneously to record the voltage signal during these tests. This process was followed for the 10 and 15 degree initial angle tests. A 5 degree initial angle test was attempted; however, due to the damping in the roll frame system, the number of complete oscillations did not reach the minimum requirement of ten full oscillations. Each test was repeated five times to investigate the repeatability of the test process. The test parameters and the results of the 10 degree and 15 degree tests are presented below.

Test Parameters for AMC-03-10:

$m_m = 10.649$ kg (model mass)

$m_p = 1.337$ kg (pendulum mass)

$h_p = 0.417$ m (distance that the pendulum mass was displaced)

Table B1 10 degree initial heel angle oscillation time measurements.

Run Description	Stop Watch No. 1 (10 oscillations) [sec]	Stop Watch No. 2 (10 oscillations) [sec]	Stop Watch Average Period [sec]	Laser Encoder [sec]
Model & Frame	24.84	24.91	2.488	2.453
Model & Frame	24.47	24.41	2.444	2.452
Model & Frame	24.93	24.16	2.455	2.451
Model & Frame	24.63	24.25	2.444	2.451
Model & Frame	24.66	24.31	2.449	2.449
AVERAGE			2.456	2.451
2 STDEV			0.037	0.003
Frame Only	19.81	19.50	1.966	1.978
Frame Only	20.15	19.60	1.988	1.978
Frame Only	19.82	19.72	1.977	1.978
Frame Only	19.75	19.82	1.979	1.978
Frame Only	19.84	19.72	1.978	1.977
AVERAGE			1.977	1.978
2 STDEV			0.016	0.001

Table B2 15 degree initial heel angle oscillation time measurements.

Run Description	Stop Watch No. 1 (10 oscillations) [sec]	Stop Watch No. 2 (10 oscillations) [sec]	Stop Watch Average Period [sec]	Laser Encoder [sec]
Model & Frame	24.40	24.25	2.433	2.454
Model & Frame	24.47	24.62	2.455	2.454
Model & Frame	24.66	24.32	2.449	2.455
Model & Frame	24.69	24.65	2.467	2.455
Model & Frame	24.50	24.56	2.453	2.455
AVERAGE			2.451	2.455
2 STDEV			0.025	0.001
Frame Only	19.94	19.87	1.991	1.978
Frame Only	19.78	19.65	1.972	1.979
Frame Only	20.03	19.69	1.986	1.979
Frame Only	19.78	19.90	1.984	1.980
Frame Only	20.00	19.81	1.991	1.980
AVERAGE			1.985	1.979
2 STDEV			0.016	0.002

The roll gyradius was calculated using Equation 22 with the measured test parameters. A general uncertainty analysis was also completed for each of the test configurations using Equation 26. The results are presented in Table B3 and Figure B6.

Uncertainty estimates in measured parameters:

$$U_{mp} = 0.001 \text{ kg}$$

$$U_{hp} = 0.002 \text{ m}$$

$$U_{mm} = 0.001 \text{ kg}$$

10 degree initial angle

$$U_{T1} = 0.037 \text{ sec (stopwatch)}$$

$U_{T2} = 0.016$ sec (stopwatch)
 $U_{T1} = 0.003$ sec (Laser encoder)
 $U_{T2} = 0.001$ sec (Laser encoder)

15 degree initial angle

$U_{T1} = 0.025$ sec (stopwatch)
 $U_{T2} = 0.016$ sec (stopwatch)
 $U_{T1} = 0.002$ sec (Laser encoder)
 $U_{T2} = 0.001$ sec (Laser encoder)

Table B3 Roll gyradius calculation results and uncertainty estimates (95% confidence level).

Run Description	Roll Gyradius [m]	Uncertainty [m]	Uncertainty [%]
Stop Watch (10 deg)	0.166	$\pm 3.10 \times 10^{-3}$	1.87
Laser Encoder (10 deg)	0.165	$\pm 4.70 \times 10^{-4}$	0.28
Stop Watch (15 deg)	0.164	$\pm 2.27 \times 10^{-3}$	1.38
Laser Encoder (15 deg)	0.166	$\pm 4.35 \times 10^{-4}$	0.26

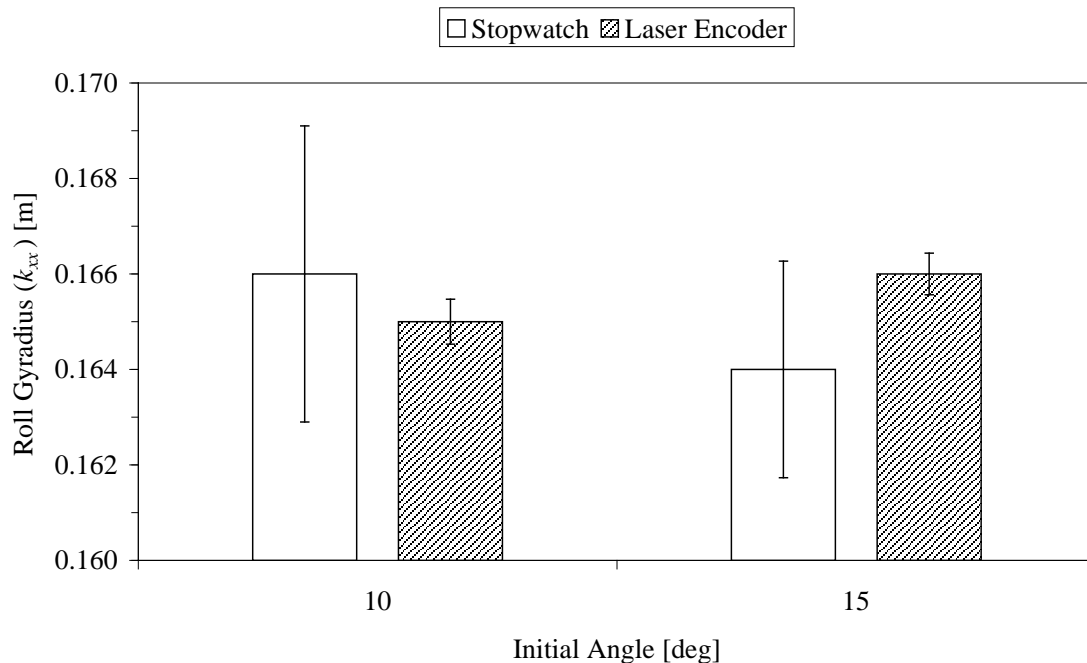


Figure B6 Roll frame test results of roll gyradius versus initial angle for the stopwatch and laser encoder measurement methods. The mean and standard deviation of all four measurements are $\mu = 0.165$ m and $\sigma = 9.57 \times 10^{-4}$ m.

The results of the roll frame tests indicate the following outcomes:

1. The laser encoder system has a significantly higher precision than the manual stopwatch method; however, the absolute values of the roll gyradius determined using the two methods are not significantly different.

2. Up to an initial angle of 15 degrees, there is no discernable effect caused by the initial angle on the measured parameters and roll gyradius.
3. The damping in the roll frame system is of a magnitude that is significant enough to require at least an initial angle of 10 degrees to achieve 10 oscillations when conducting a test using the small roll frame.

B.2. Comparison with CAD Method

As discussed in § B.1, the geometry of the pontoon model was modelled using the Rhinoceros 3D CAD software program. The pontoon was modelled as a series of solid elements based on a metrological survey conducted by the author. The physical model is manufactured with a plywood substrate covered externally with a fibreglass laminate and internally with an epoxy lacquer. The internal stiffeners are glued to the external panels and are only covered with the epoxy lacquer. Despite the relative difference in the density of the materials and coatings, the CAD model is an isotropic representation of the physical geometry of the pontoon. The volume properties of the model were calculated using the *VolumeMoments* function with all of the solid objects selected. The volume moment data returned by Rhinoceros 3D and relevant to this study are summarised in Table B4 below. These values are stated relative to the model's geometric centre of volume.

Table B4 Rhinoceros 3D calculated volume moment data.

Calculated Property	Calculated Value	Calculated Error
Cumulative Volume [m ³]	0.017	$\pm 1.60 \times 10^{-8}$
Volume Moment About Centroid (I_x) [m ⁵]	4.75×10^{-4}	$\pm 1.60 \times 10^{-9}$
Volume Gyraadii About Centroid (k_{xx}) [m]	0.167	$\pm 3.70 \times 10^{-7}$
Longitudinal Volume Centroid (XCG) [m]	0.669	$\pm 1.20 \times 10^{-6}$
Transverse Volume Centroid (YCG) [m]	-3.38×10^{-6}	$\pm 8.80 \times 10^{-9}$
Vertical Volume Centroid (ZCG) [m]	0.108	$\pm 2.70 \times 10^{-7}$

Based on the results presented in Table B3 and Table B4 there is a 1.20 percent difference between the mean roll gyradius value measured using the roll frame and the roll gyradius calculated using the CAD method. Considering the uncertainties in the physical measurement and the assumptions of homogeneity and isotropy in the CAD model, this result indicates that the roll frame has provided an accurate measurement of the roll gyradius for the pontoon model in air.

B.3. Design Issues

The AMC currently operates two roll frame devices to measure the roll gyradius of model marine craft and offshore structures. A larger roll frame exists in addition to the small roll frame evaluated in this investigation. The requirement to have two roll frames is driven by the overall size of the model being tested. To date, the operators have noted several potential issues that may influence the roll gyradius measurement [15]. These issues are:

1. The deflection of the dynamic frame's longitudinal beams due to the weight of the model and the resulting misalignment of the roll frame axis of rotation and the model's vertical centre of mass.
2. Misalignment of the shaft axes, independent of loading, which may introduce excessive friction damping and limit the duration of oscillation.

These issues have been investigated, albeit at a cursory level, to verify their potential for introducing error into the roll frame roll gyradius measurement system. A finite element structural analysis was completed for the small and large roll frames to quantify the effect of model weight on the deflection of the dynamic frame sub-assembly. The analysis and results are presented in § B.3.1. A qualitative evaluation of the bearings has been completed and alternative options are presented in § B.3.2.

B.3.1 Misalignment due to structural deflection

A linear structural finite element (FE) analysis of the dynamic frame sub-assembly was completed using the Maestro V11.0.0 FE analysis software [16] for both the small and large roll frames used by the AMC. In both cases, the dynamic frame geometry was modelled and meshed using Rhinoceros 3D and Maestro. The dynamic frame was modelled using shell elements only. Restraints were placed on the frame at the location of the axis of rotation on each transverse beam. The frame was restrained such that no vertical (z) or longitudinal (x) translation or rotation was permitted. Four point loads were placed at the location of the underslung supports in their innermost location. Each point load carries one quarter of the total applied load.

The Maestro mesh generated for the small roll frame is presented in Figure B7. The mesh contains 1385 nodes and 1350 triangular elements and is relatively coarse. The material properties assigned to the structural model are presented in Table B5.

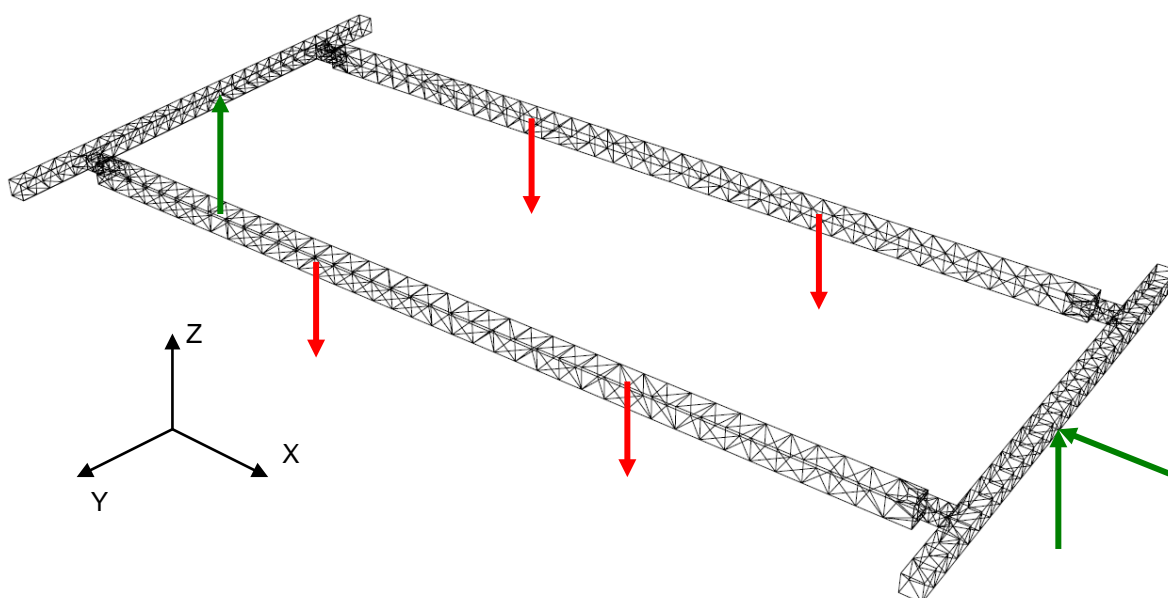


Figure B7 AMC small roll frame: dynamic frame FE mesh geometry, point loads (red arrows) and restraints (green arrows).

Table B5 Material properties assigned to the small roll frame FE model.

Property	Value
Material	Aluminium
Wall thickness of SHS	1.50 mm
Young's Modulus of Elasticity	70 GPa
Poisson's Ratio	0.33

A load versus deflection analysis was completed for the small roll frame for model weights of between 10 kilograms and 100 kilograms inclusive. The FE analysis results indicate that the location of maximum deflection (and absolute displacement) occurs at the mid-span of the longitudinal beams (Figure B8). This is also the location of the maximum combined stress (Figure B9). The load versus deflection results for the small roll frame is presented in Table B6. The results indicate that there is negligible deflection in the frame for models weighing up to 50 kilograms. At loads above 50 kilograms the amount of deflection and misalignment begins to exceed the acceptable manufacturing tolerances that are applied to physical model itself. The ITTC prescribes a maximum dimensional manufacturing tolerance of ± 1.00 millimetre [17]. It is in this region where the misalignment of the model's centre of mass and the roll frame roll axis could introduce measurement errors in the parameters used to calculate the model's roll gyradius.

Table B6 AMC small roll frame: model weight versus longitudinal beam maximum deflection.

Model Weight [kg]	Longitudinal Beam Maximum Deflection [mm]
10	0.18
20	0.37
30	0.55
40	0.73
50	0.92
60	1.10
70	1.28
80	1.47
90	1.65
100	1.84

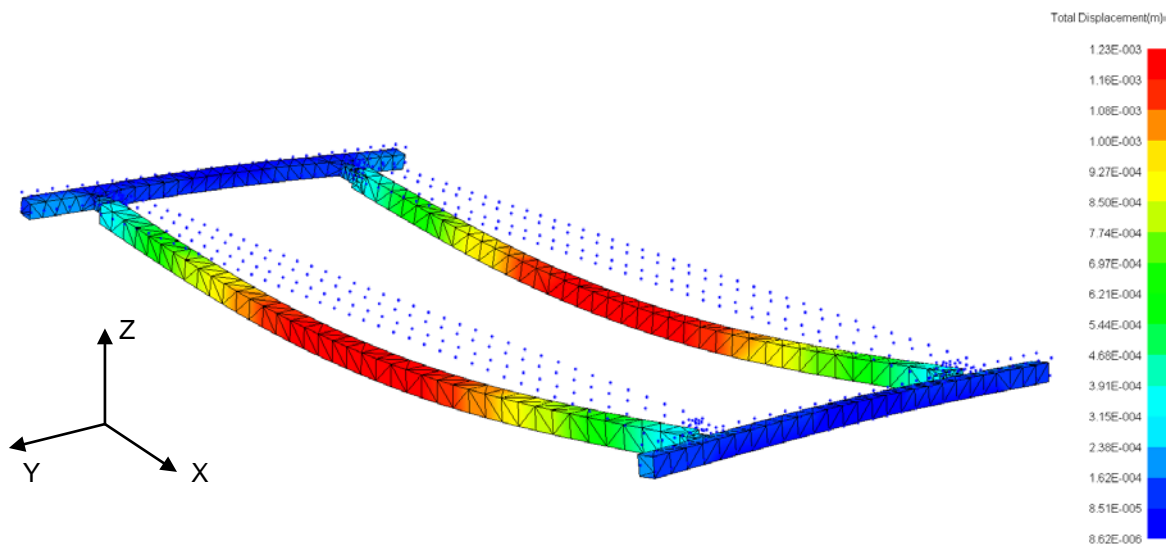


Figure B8 Beam deflection due to four point loads and a model mass of 60kg. The original (unloaded) frame position is represented by the array of markers. The displacement is scaled by a factor of 100. In this condition the maximum displacement is 1.10 millimetres and occurs at the mid-span of the two longitudinal beams.

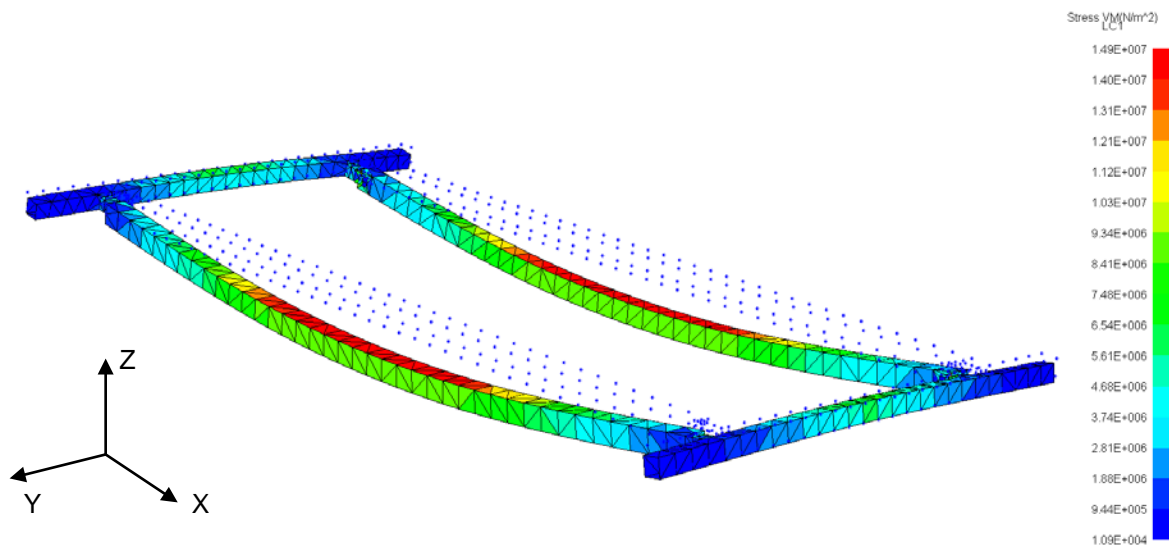


Figure B9 Colour map of the Von Mises combined stress distribution due to four point loads and a model mass of 60kg. The original (unloaded) frame position is represented by the array of markers.

The FE mesh model of the large roll frame's dynamic frame assembly is substantially finer than that developed for the small roll frame. This is simply due to the geometry discretization process used to achieve elements with an aspect ratio as close to unity as possible. The model comprises 4316 nodes and 4298 quadrilateral elements. The material properties of the large roll frame's structural sections, and those used in the FE analysis, are the same as the small roll frame (Table B5). The maximum model length and breadth that can be accommodated by the large roll frame is 2.5 metres and 0.75 metres, respectively.

A load versus deflection analysis was completed for the large roll frame for model weights of between 20 kilograms and 120 kilograms inclusive. The FE analysis results indicate that, similar to the small roll frame, the location of maximum deflection occurs at the mid-span of the longitudinal beams (Figure B10). This is also the location of the maximum combined stress (Figure B11). The load versus deflection results for the small roll frame is presented in Table B7. The results indicate that even for a model of 20 kilograms, the deflection exceeds the maximum dimensional tolerance for model manufacture. For a model weight of 120 kilograms the deflection in the longitudinal beam is significant (5.36 millimetres over a span of 1310 millimetres). It is very likely that the deflection of the longitudinal beams and the resulting misalignment of the model's centre of mass and the roll frame roll axis will introduce non-negligible measurement errors in the measurement of the model's roll gyradius.

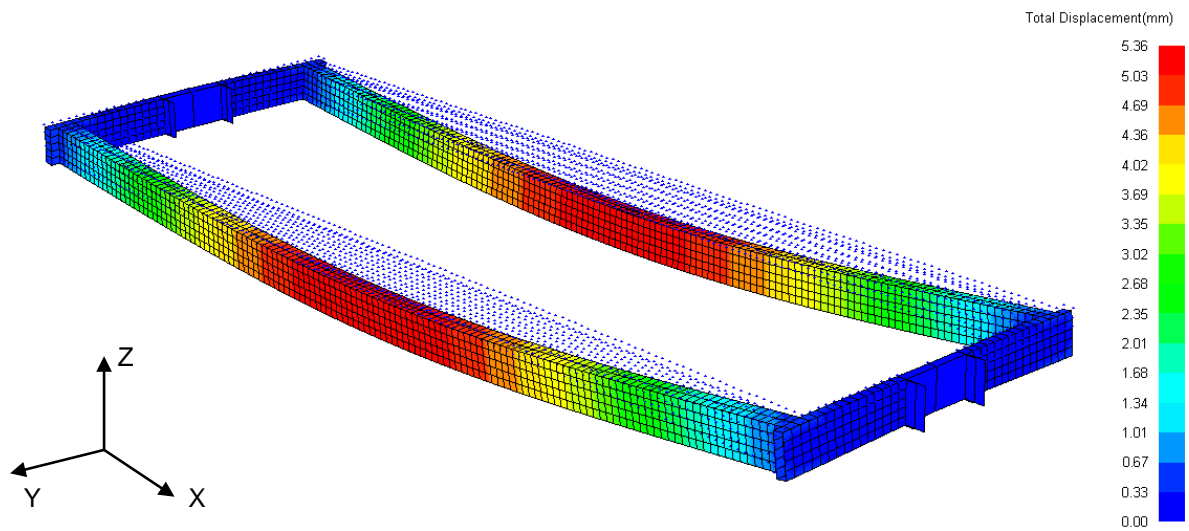


Figure B10 Large roll frame dynamic frame assembly: beam deflection due to four point loads and a model mass of 120 kg. The original (unloaded) frame position is represented by the array of markers. The displacement is scaled by a factor of 100. In this condition the maximum displacement is 5.36 millimetres and occurs at the mid-span of the two longitudinal beams.

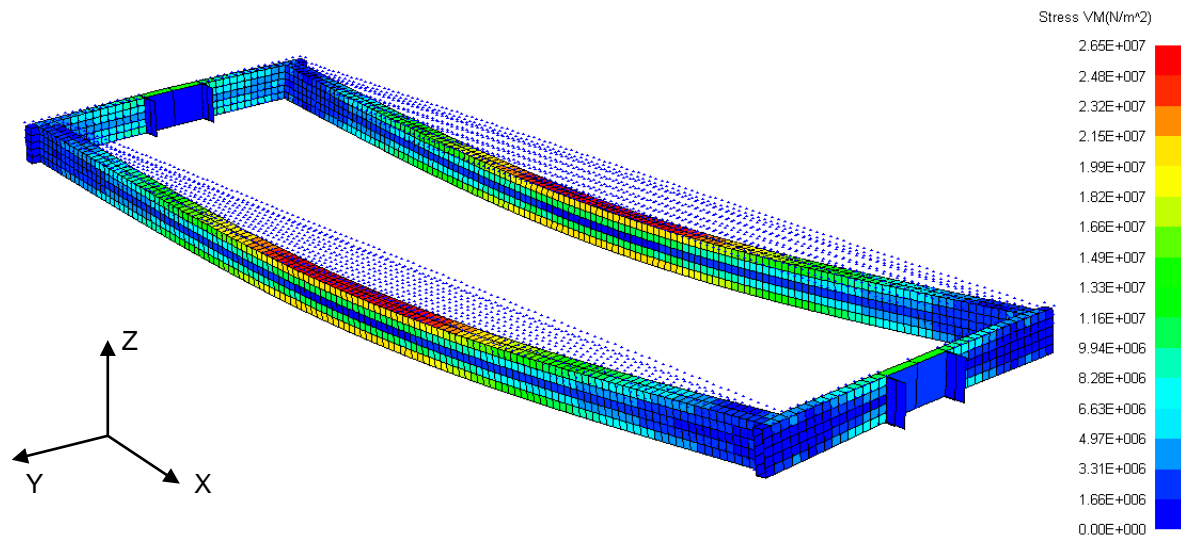


Figure B11 Large roll frame dynamic frame assembly: colour map of the Von Mises combined stress distribution due to four point loads and a model mass of 120 kg. The original (unloaded) frame position is represented by the array of markers. The displacement is scaled by a factor of 100.

Table B7 AMC small roll frame: model weight versus longitudinal beam maximum deflection.

Model Weight [kg]	Longitudinal Beam Maximum Deflection [mm]
20	1.04
40	1.91
60	2.77
80	3.64
100	4.50
120	5.36

As discussed in § 4.1.1, it is important to maintain a very light dynamic frame in order to maximise the difference in the moments of inertia of the frame only and frame with model test configurations to minimise the uncertainty in the measurement of the roll gyradius. Achieving this weight requirement and maintaining the structural integrity of the frame is considered to be a challenging design problem and one that must be addressed through material selection and/or structural arrangement. This task is beyond the scope of this investigation. Furthermore, the FE analyses presented in this report are considered to be of a preliminary level. It would be prudent to conduct more detailed analyses that give consideration to the dynamic loads acting on the entire roll frame system when in operation. Nonetheless, the preliminary FE analysis results provide evidence that the dynamic frame and model will be misaligned under normal operating conditions.

B.3.2 Shaft and Bearing Misalignment

In general terms, shaft and bearing misalignment, whether angular or parallel, will result in dysfunctional operation and unnecessary wear. While some bearing types can accommodate small levels of angular misalignment, the misalignment of the shaft is the critical issue in the case of the roll frame. Moreover, the freedom of the bearing to accommodate misalignment acts in opposition to maintain precise shaft alignment. The two major operational dysfunctions that result due to shaft misalignment are:

1. The centre of mass of the model is not aligned with the roll frame's axis of rotation.
2. There is an increase in the system damping which affects the operability of the roll frame

Depending on the severity of the shaft misalignment, these dysfunctions will directly affect the measurement of the roll periods (T_1 and T_2) and the consequently, the roll gyradius (k_{xx}).

The small roll frame's shaft and bearing arrangement is shown in Figure B12.

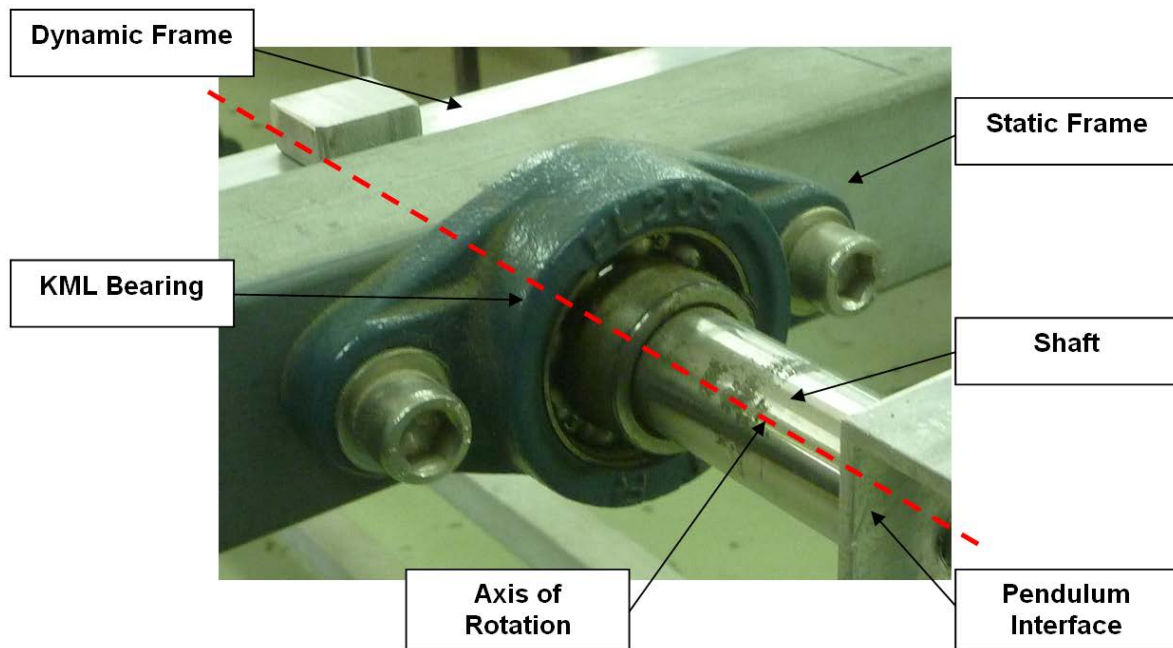


Figure B12 KML mounted flange bearing and shaft arrangement connecting the static and dynamic frame sub-assemblies.

An alternate design solution and one that has been used in a similar application is the knife edge mounting arrangement shown in Figure B13. If integrated effectively, the knife edge arrangement results in a durable coupling that will allow the dynamic frame to rotate about its longitudinal axis with minimal friction losses. Referring to Figure B1, the vertical ($z-z$), lateral ($y-y$) and yaw (rotation about $z-z$) alignment of the knife edge axes is achieved by aligning the knife edge and seat components at both ends of the roll frame. Rotation about the $y-y$ axis (the condition where the knife edge and seat break contact with each other) is limited by the weight of the frame and the structural rigidity inherent in a sufficiently well designed seat and dynamic sub-assembly.

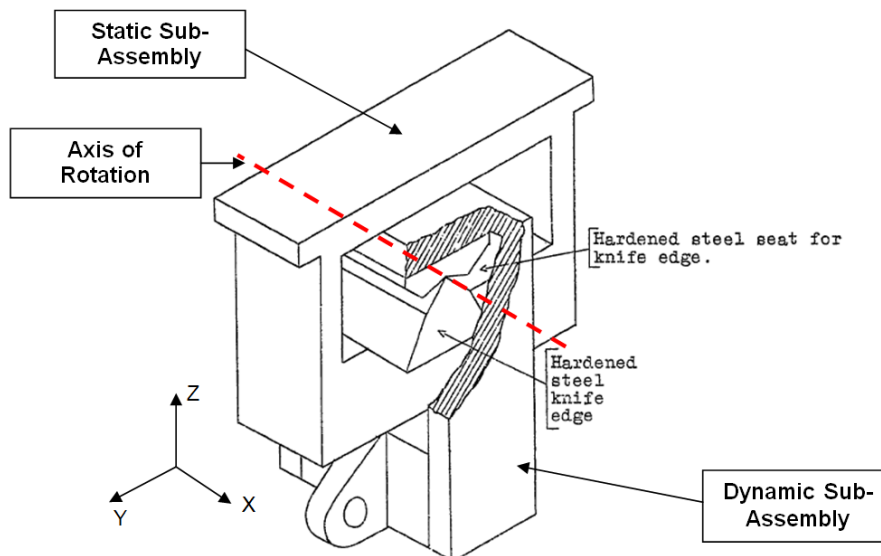


Figure B13 Knife edge mounting arrangement presented by Miller [18].

B.4. Summary

The function and performance evaluation completed for the AMC roll frame has resulted in the following outcomes:

1. The quantitative tests conducted using the small roll frame with the simple pontoon model indicate that while measuring the roll period using the integrated laser encoder system is more precise than the manual stopwatch method, it is not significantly more accurate. The significant benefit of using the integrated laser encoder system is its reliability and therefore the need to only conduct one oscillation test for each frame and model configuration as opposed to multiple manual stopwatch tests.
2. In this instance (testing the relatively light pontoon model) the result of the roll frame test using the small roll frame provided an accurate roll gyradius result based on the comparison with a three-dimensional solid CAD model calculation.
3. There is considerable damping in the small roll frame system that prohibited testing with initial angles on inclination below 10 degrees.
4. A preliminary structural analysis of the dynamic frame assembly of the small and large roll frames used by the AMC has indicated that the structural design of the large roll frame will result in a misalignment of the model and the roll frame axis of rotation under normal operating conditions. Misalignment will also occur for the small roll frame; however, for the weight range of the models commonly tested in this device the effects are not likely to be significant. Nonetheless, further analyses that consider dynamic loading effects and that assess the entire frame assembly and modes of distortion are recommended.
5. Although not considered to be a significant contributor to the measurement error in the small roll frame, the issue of shaft and bearing misalignment in the large roll frame and its effects could be resolved through the use of a knife edge type coupling.

Appendix C: General Uncertainty Analyses: Derivation of Error Propagation Equations

C.1. Roll Frame Test: Roll Gyradius (in air)

Partial derivatives of data reduction equation (Equation 17):

$$\frac{\partial k_{xx}}{\partial m_p} = \frac{1}{2} \cdot \frac{1}{\sqrt{\frac{g \cdot m_p \cdot h_p \cdot (T_2^2 - T_1^2)}{4\pi^2 m_m}}} \cdot \frac{g \cdot h_p \cdot (T_2^2 - T_1^2)}{4\pi^2 m_m} \quad \text{Equation 39}$$

$$\frac{\partial k_{xx}}{\partial h_p} = \frac{1}{2} \cdot \frac{1}{\sqrt{\frac{g \cdot m_p \cdot h_p \cdot (T_2^2 - T_1^2)}{4\pi^2 m_m}}} \cdot \frac{g \cdot m_p \cdot (T_2^2 - T_1^2)}{4\pi^2 m_m} \quad \text{Equation 40}$$

$$\frac{\partial k_{xx}}{\partial T_1} = \frac{1}{2} \cdot \frac{1}{\sqrt{\frac{g \cdot m_p \cdot h_p \cdot (T_2^2 - T_1^2)}{4\pi^2 m_m}}} \cdot \frac{g \cdot m_p \cdot h_p \cdot (T_2^2 - 2T_1)}{4\pi^2 m_m} \quad \text{Equation 41}$$

$$\frac{\partial k_{xx}}{\partial T_2} = \frac{1}{2} \cdot \frac{1}{\sqrt{\frac{g \cdot m_p \cdot h_p \cdot (T_2^2 - T_1^2)}{4\pi^2 m_m}}} \cdot \frac{g \cdot m_p \cdot h_p \cdot (2T_2 - T_1)}{4\pi^2 m_m} \quad \text{Equation 42}$$

$$\frac{\partial k_{xx}}{\partial h_p} = \frac{1}{2} \cdot \frac{1}{\sqrt{\frac{g \cdot m_p \cdot h_p \cdot (T_2^2 - T_1^2)}{4\pi^2 m_m}}} \cdot \frac{-g \cdot m_p \cdot (T_2^2 - T_1^2)}{4\pi^2 m_m} \quad \text{Equation 43}$$

C.2. Inclining Test: Metacentric Height

Partial derivatives of data reduction equation (Equation 25):

$$\frac{\partial GM_T}{\partial m} = \frac{d}{M \cdot \tan \theta} \quad \text{Equation 44}$$

$$\frac{\partial GM_T}{\partial d} = \frac{m}{M \cdot \tan \theta} \quad \text{Equation 45}$$

$$\frac{\partial GM_T}{\partial M} = -\frac{m \cdot d}{M^2 \cdot \tan \theta} \quad \text{Equation 46}$$

$$\frac{\partial GM_T}{\partial \theta} = -\frac{m \cdot d}{M \cdot (\sec^2 \theta)^2} = -\frac{m \cdot d}{M \cdot (1 + \tan^2 \theta)^2} \quad \text{Equation 47}$$

C.3. Roll Decay Test: Roll Gyradius (in water)

Partial derivatives of data reduction equation (Equation 23):

$$\frac{\partial k_{xx}''}{\partial T_\phi} = \frac{\sqrt{g \cdot GM_T}}{2\pi} \quad \text{Equation 48}$$

$$\frac{\partial k_{xx}''}{\partial GM_T} = \frac{T_\phi \cdot \sqrt{g}}{2\pi \cdot \sqrt{GM_T}} \quad \text{Equation 49}$$

DEFENCE SCIENCE AND TECHNOLOGY ORGANISATION DOCUMENT CONTROL DATA						
					1. DLM/CAVEAT (OF DOCUMENT)	
2. TITLE An Investigation into the Effects of Roll Gyradius on Experimental Testing and Numerical Simulation: Troubleshooting Emergent Issues				3. SECURITY CLASSIFICATION (FOR UNCLASSIFIED REPORTS THAT ARE LIMITED RELEASE USE (L) NEXT TO DOCUMENT CLASSIFICATION) Document (U) Title (U) Abstract (U)		
4. AUTHOR(S) Edward Dawson				5. CORPORATE AUTHOR DSTO Defence Science and Technology Organisation 506 Lorimer St Fishermans Bend Victoria 3207 Australia		
6a. DSTO NUMBER DSTO-TN-1402		6b. AR NUMBER AR-016-225		6c. TYPE OF REPORT Technical Note		7. DOCUMENT DATE January 2015
8. FILE NUMBER 2014/1106877/1	9. TASK NUMBER 07-359	10. TASK SPONSOR DGNPS		11. NO. OF PAGES 51		12. NO. OF REFERENCES 18
13. DSTO Publications Repository http://dspace.dsto.defence.gov.au/dspace/			14. RELEASE AUTHORITY Chief, Maritime Division			
15. SECONDARY RELEASE STATEMENT OF THIS DOCUMENT <i>Approved for public release</i>						
OVERSEAS ENQUIRIES OUTSIDE STATED LIMITATIONS SHOULD BE REFERRED THROUGH DOCUMENT EXCHANGE, PO BOX 1500, EDINBURGH, SA 5111						
16. DELIBERATE ANNOUNCEMENT No Limitations						
17. CITATION IN OTHER DOCUMENTS Yes						
18. DSTO RESEARCH LIBRARY THESAURUS Roll Gyradius, Roll Frame Test, Ship Motion Simulation, Roll Decay						
19. ABSTRACT This report presents the analyses, results and recommendations of an investigation into the specification and determination of a platform's roll radius of gyration and its influence on the measured or predicted roll response of a maritime platform. The investigation and report seek to resolve known deficiencies in the specification and determination of roll radius of gyration and provide direct guidance and supporting information to the experimenter and analyst to support ship motion analysis. Three solution sets were developed based on the results of the investigation. The solutions include: the establishment of a method of specifying roll radius of gyration requirements, the development of a decision tree tool to guide the analyst to the appropriate method of determining the roll radius of gyration and a set of system level technology solutions that enable the roll radius of gyration to be determined for model scale, full scale and virtual maritime platforms.						